Recent results on ultra-peripheral collisions measured with ALICE

Adam Matyja
Institute of Nuclear Physics
Polish Academy of Sciences, Kraków

Białasówka seminar
Kraków

14 June 2024, Kraków

Outline

- Introduction
- Experimental apparatus in Run 2 and Run 3
- Mesurements
  - Photoproduction of K^+K^- pairs from Run 2
  - Azimuthal anisotropy from quantum interference in ρ^0 photoproduction from Run 2
  - Four pion analysis photoproduction in Pb-Pb from Run 2
  - Vector mesons (ρ^0 and J/ψ) in UPC in Run 3
- FOCAL detector upgrade at IFJ PAN, Kraków
- Summary

Ultra-peripheral collisions (UPC)

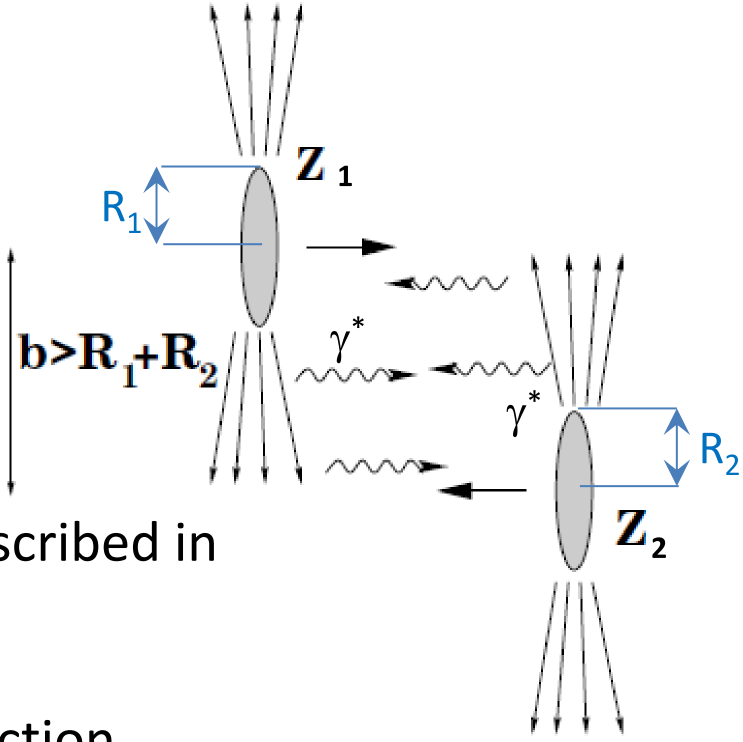

- Impact parameter $b > R_1 + R_2$
  - Hadronic interactions suppressed
- Photon induced reactions:
  - A flux of quasi-real photons well described in Weizsäcker-Williams approximation
  - Photon flux $\sim Z^2$ ($Z_{Pb} = 82$)
  - Large γ-induced interaction cross section
- Clear signature:
  - Low detector activity
  - Rapidity gap(s)

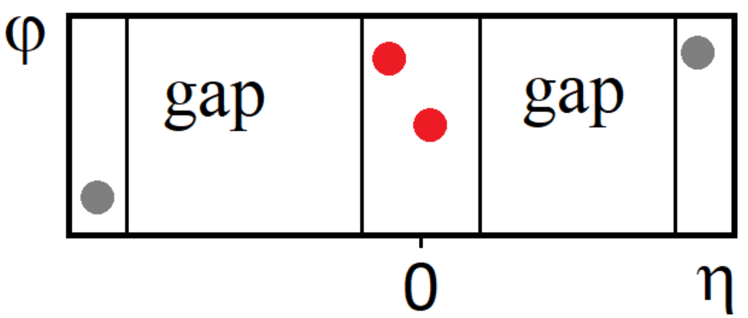

Photoproduction and main variables

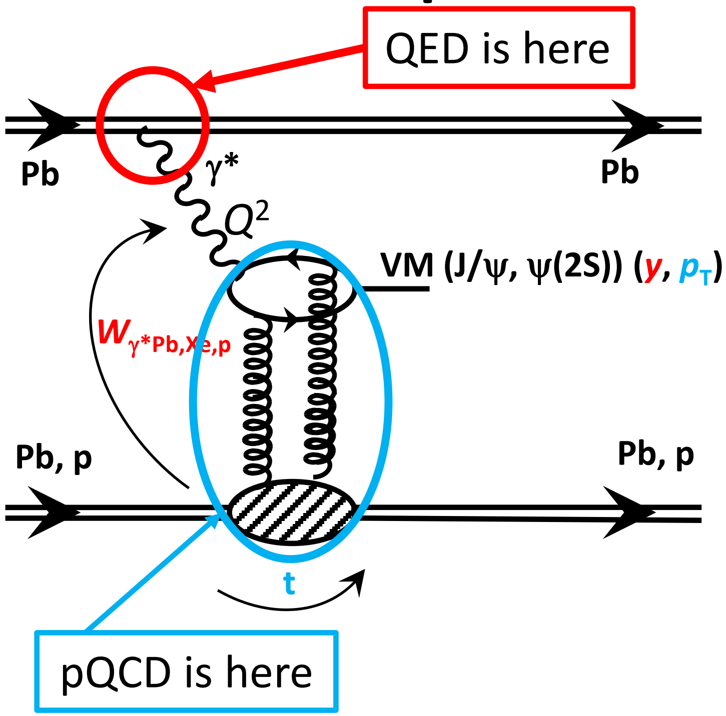

- **Coherent**:
  - Photon couples coherently to all nucleons (whole nucleus)
  - $\langle p_T^{VM} \rangle \sim 1/R_{Pb} \sim 50$ MeV/c
- **Incoherent**:
  - Photon couples to a single nucleon
  - $\langle p_T^{VM} \rangle \sim 1/R_p \sim 400$ MeV/c

- Photon $Q^2 \sim M_{VM}^2 / 4$
  - Hard scale - high mass of J/ψ
  - Semi-hard scale for ρ^0
- Vector Meson (VM) quantum numbers:
  - $J^{PC} = 1^{--}$
- Bjorken-x: fraction of longitudinal momentum of proton

$$x_B = \frac{M_{VM}}{\sqrt{s_{NN}}} e^{\pm y}$$

  - Photoproduction is sensitive to gluon density evolution at low x_B at LO
  - There are new NLO calculations
- Photon-target center-of-mass energy

$$W^2_{\gamma^* Pb,p} = 2E_{Pb,p} M_{VM} e^{\mp y}$$

- 4-momentum transfer t
  - Gluon distribution in the transverse plane $|t| \sim p_T^2$

Motivation

- **Coherent** vector meson (ρ^0, J/ψ) **photoproduction** particularly sensitive to the **gluon shadowing**
- $|t|$-dependence helps to constrain **transverse gluonic** structure at low x_B and is sensitive to the gluon **saturation**
- The interference is sensitive to the **gluon distribution** and to the size of nuclei $\rightarrow$ gluon tomography
- Possibility of studies features of not well known **resonances**
- Constrain parameters of **models**

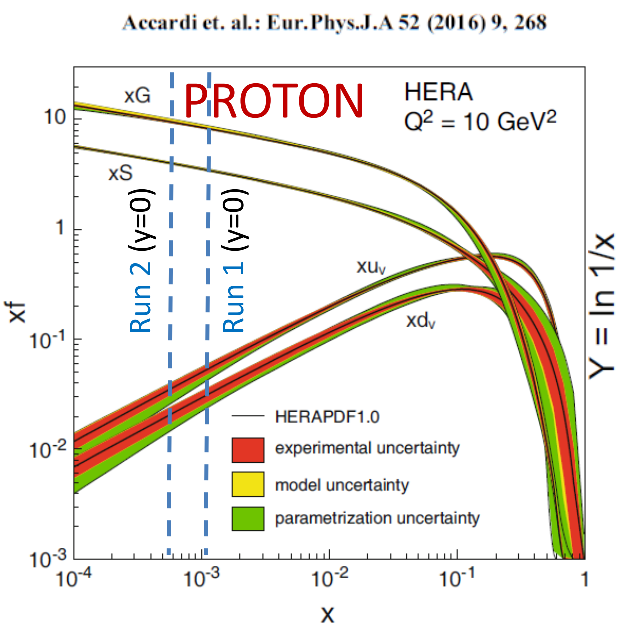

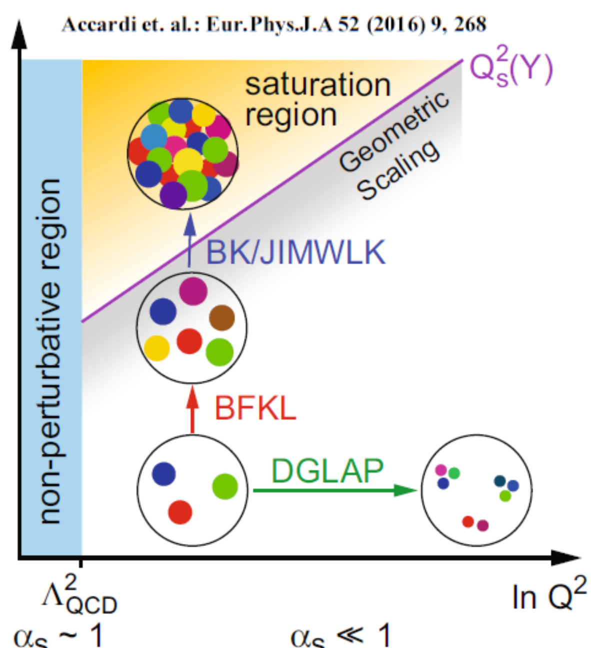

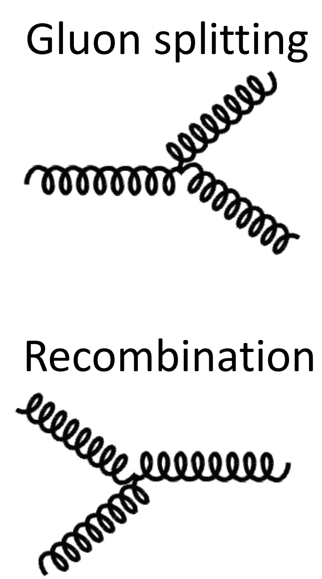

ALICE: *JINST* **3** S08002 (2008) ;
Int. J. Mod. Phys. A29 (2014) 1430044

ALICE in Run 2

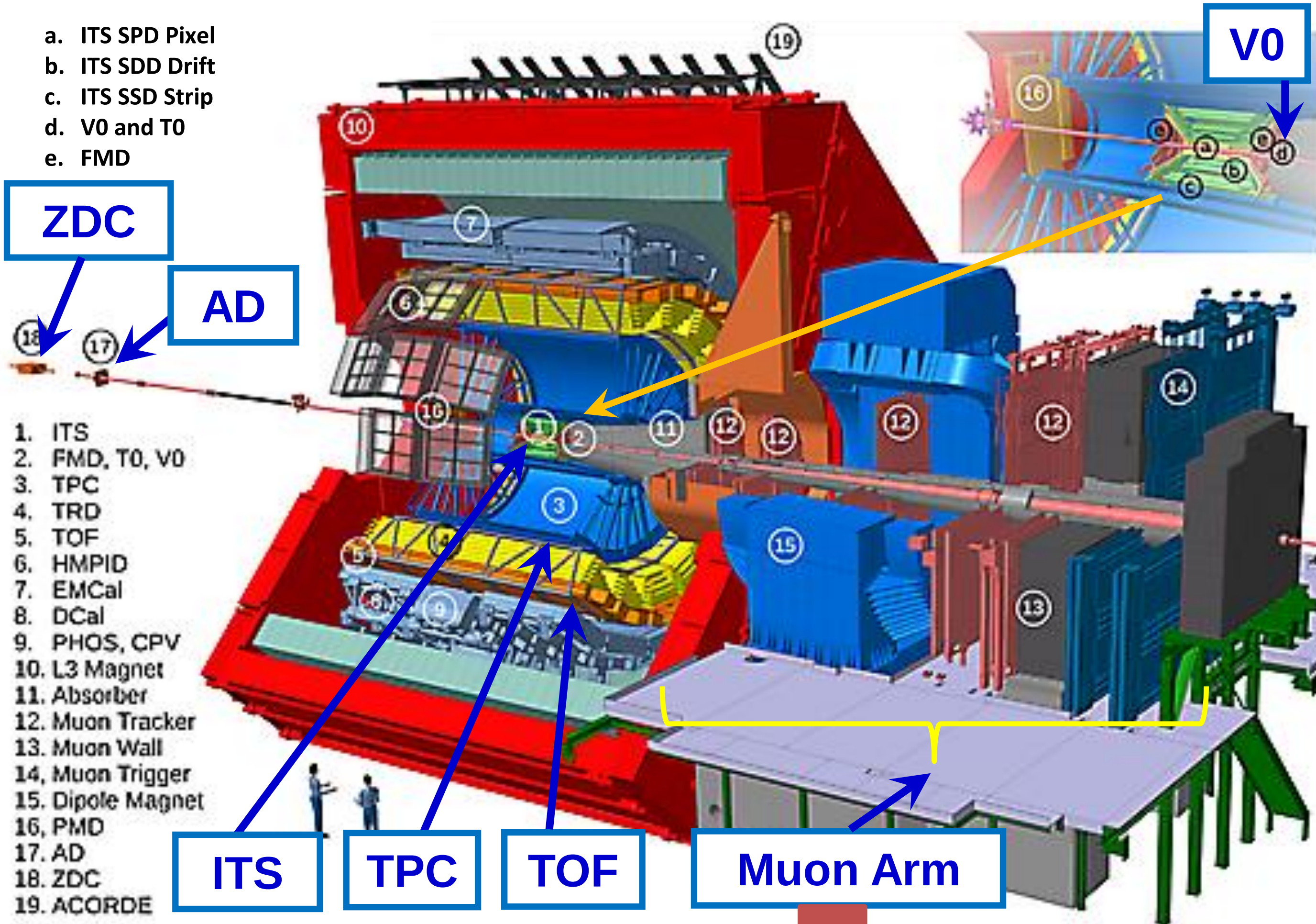

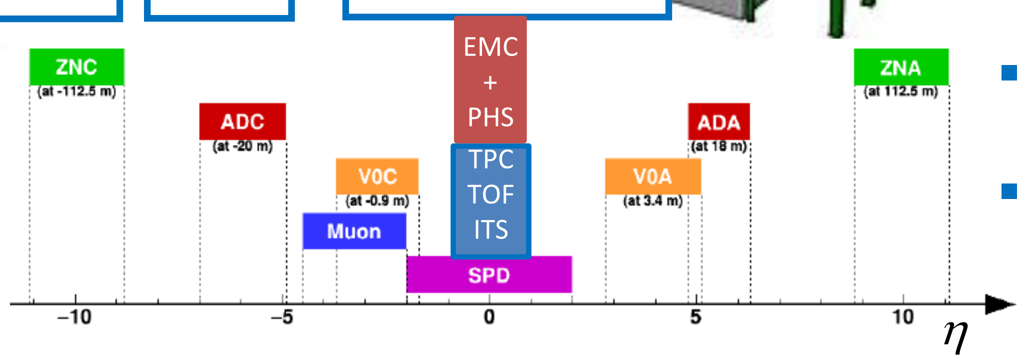

- **Central Barrel tracking ($e^{\pm}$, $h^{\pm}$)**
  - $|\eta| < 0.9$, $0 < \varphi < 2\pi$
  - ITS - silicon detector
  - TPC - gas drift detector
  - TOF - resistive plate chambers
- **Forward tracking ($\mu^{\pm}$)**
  - $-4 < \eta < -2.5$
  - Absorber
  - Muon tracker
  - Muon trigger
  - Dipole magnet
- **Diffractive detectors**
  - AD - scintillator counter
  - V0 - scintillator counter
  - ZDC - sampling calorimeter
- **Vertex**
  - Pixel
- **Trigger**
  - SPD, TOF, AD, V0, Muon

ALICE in Run 3

ALICE: *JINST* 19 P05062 (2024)

- Large **upgrade** during LS2
  - Inner Tracking System – full pixel layers
  - Time Projection Chamber – GEM readout
  - New Muon Forward Tracker
  - New Fast Interaction Trigger (FV0 + FT0 + FDD)
  - New Event Processing Nodes Farm
  - Upgraded readout for most of detectors
  - ⇒ **continous readout** at high rate

- **pp data** taking at 500 kHz
  - Temporary data storage on disk buffer
  - **Asynchronous (offline) trigger** with $\sim 10^{-4}$ selection

- **Pb-Pb data** taking at 50 kHz
  - **All Compressed Time Frames data stored** on tape

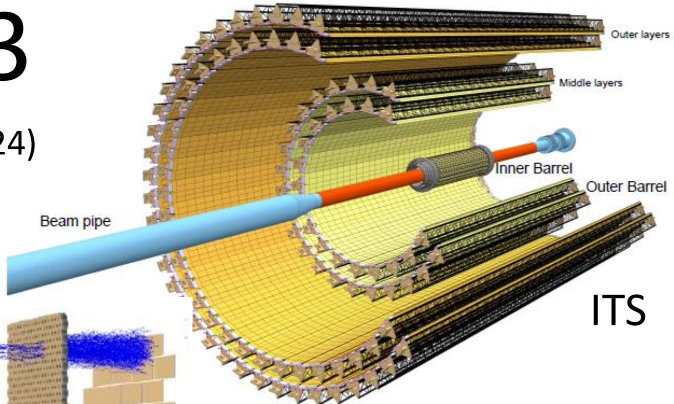

ITS

TPC

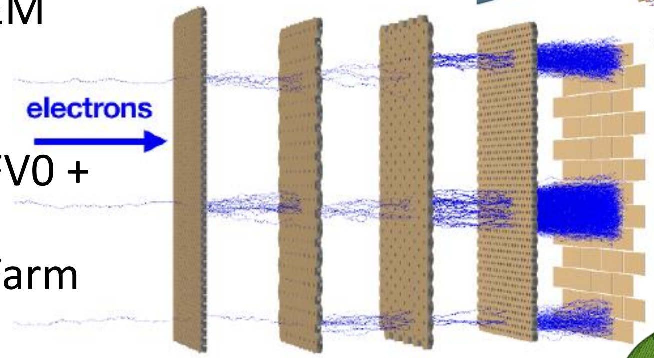

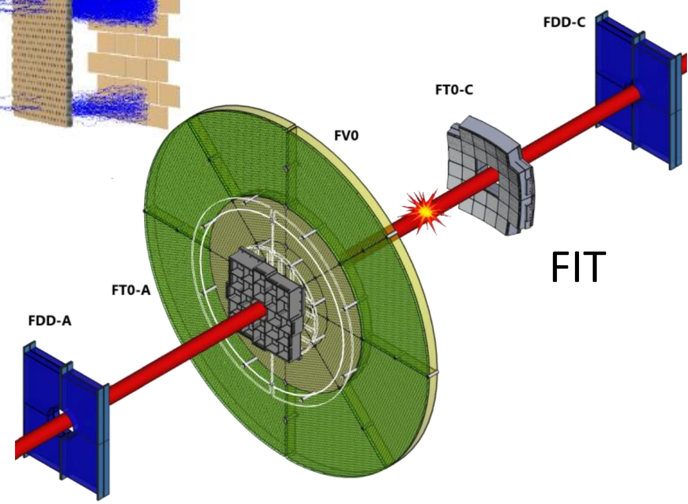

FIT

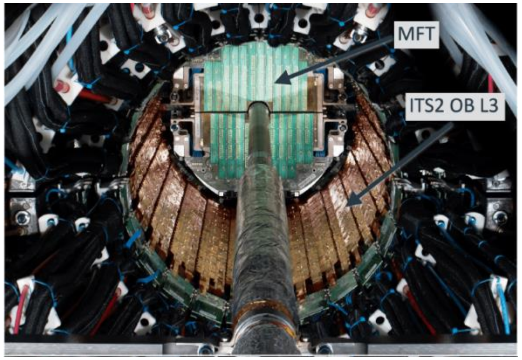

Exclusive K^+K^- photoproduction

- Different physics processes
  - Non distinguishable
  - Interfere
- BR(ϕ(1020) $\rightarrow K^+K^-$) = 49.2 %
- Cross section described by Söding formula

$$\frac{d\sigma}{dM_{KK}} = \left| A_\phi \frac{\sqrt{M_{KK} M_\phi \Gamma_\phi}}{{M_{KK}}^2 - {M_\phi}^2 + i M_\phi \Gamma_\phi} + B_{KK} \right|^2$$

$$\Gamma_\phi = \Gamma_0 \frac{M_K}{M_{KK}} \left(\frac{{M_{KK}}^2 - 4{M_K}^2}{{M_\phi}^2 - 4{M_K}^2} \right)^{3/2}$$

Native ϕ width: $\Gamma_0 = 4.249 \pm 0.013$ MeV/c^2

ϕ(1020) photoproduction

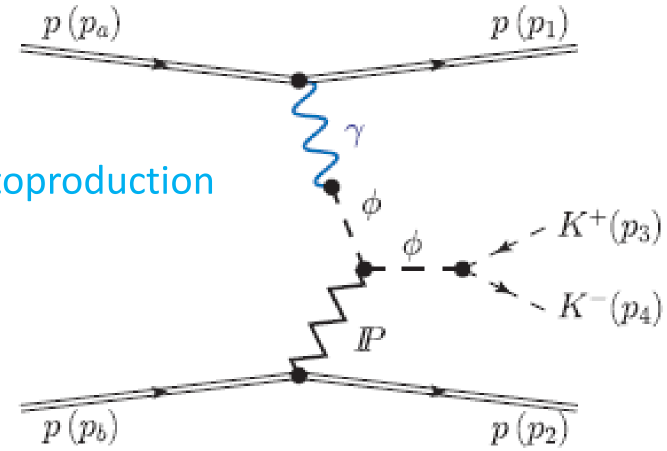

Continuum of nonresonant (Drell-Söding)

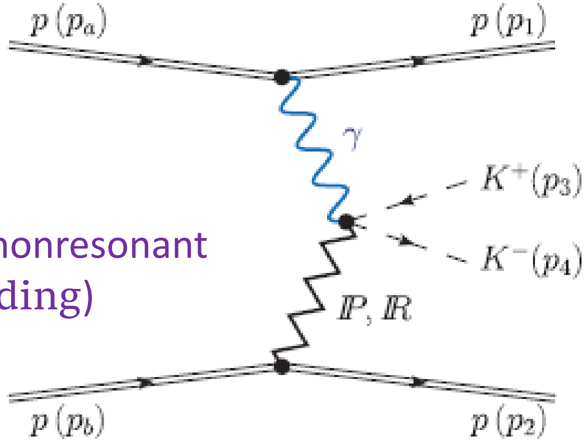

Diagrams from P. Lebiedowicz et al., PRD 98, 014001 (2018)

- Tool to access coulplings of vector meson (ϕ(1020)) and meson pairs (K^+K^-) with a photon and a nucleus at extremely high energies

Exclusive K^+K^- photoproduction

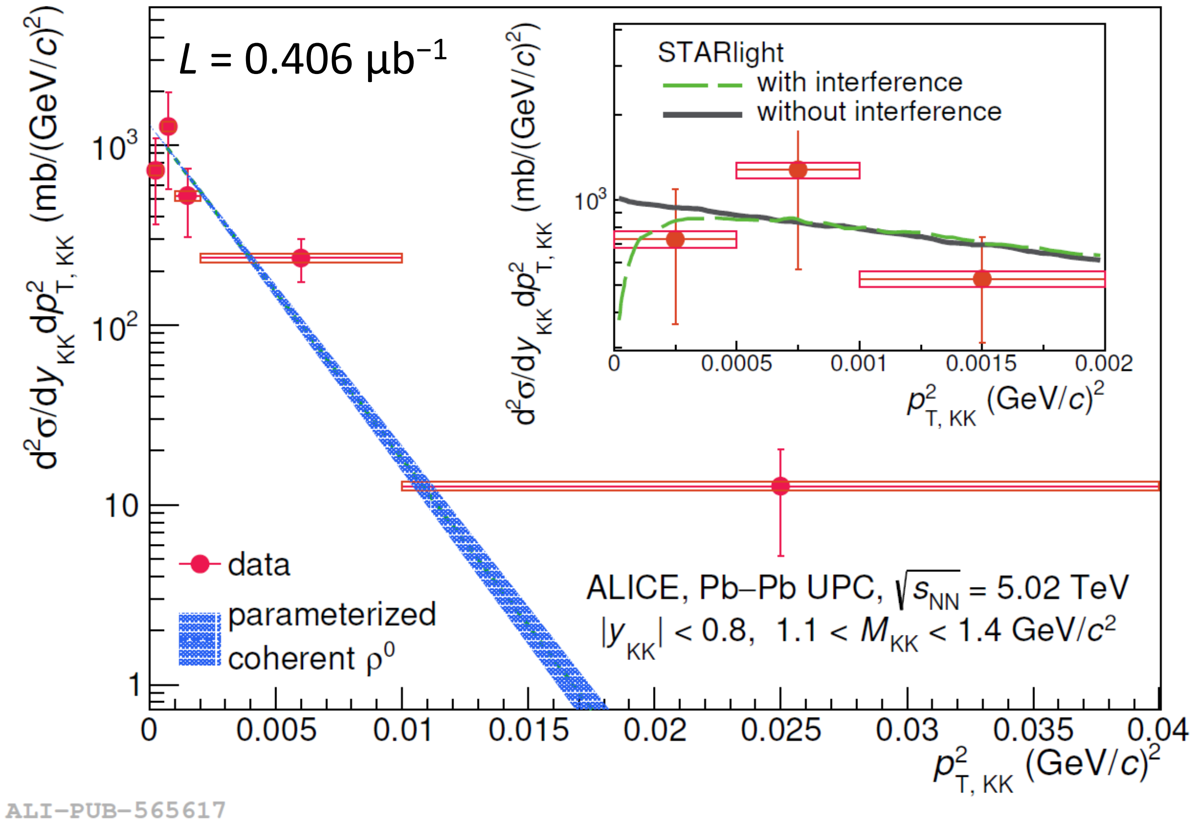

ALICE: PRL 132, 222303 (2024)

- $f(p_T^2) = A \exp(-B\, p_T^2)$
- Slope parameter

$B = 428 \pm 6^{stat} \pm 15^{syst}$ $(\mathrm{GeV}/c)^{-2}$ taken from ALICE measurement

- First measurement of K^+K^- photoproduction in heavy-ion UPCs
- Exclusive K^+K^- photoproduction as a function of $p_T^2 \approx |t|$
- Well described by exponential function with ALICE parameters
- The cross section at low p_T^2 is in favor of photoproduction with destructive interference (observed by STAR, PRL 102, 112301 (2009))

Inv. mass of coherent K^+K^- photoproduction

- Photon-nucleus center of mass energy $W_{\gamma\mathrm{Pb}}$ varies from 33 to 188 GeV
  - Order of magnitude higher than previous measurements
- Contribution from $\gamma\gamma \rightarrow X \rightarrow K^+K^-$ negligible
- Söding formula with $|B/A|$ = 0 hypothesis is 2σ away from the measurement

$\Rightarrow$ non-negligible non-resonant contribution

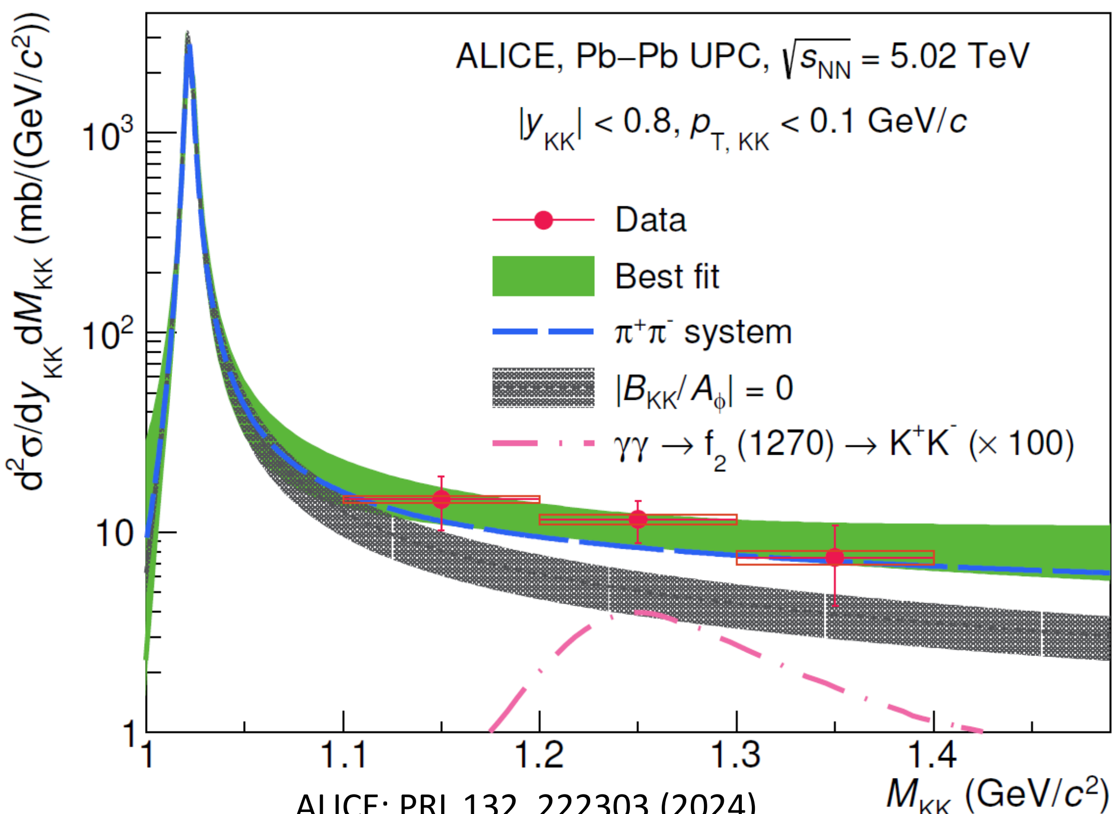

I-PUB-565621

ALICE: PRL 132, 222303 (2024)

The measured M_{KK} distribution in agreeement with ϕ resonance + continuum production

Integrated cross section
$d\sigma/dy_{\mathrm{KK}} = 3.37 \pm 0.61^{\mathrm{stat}} \pm 0.15^{\mathrm{syst}}$ mb

Best fit:
$|B_{\mathrm{KK}}/A_\phi|$ = 0.28 (GeV/c^2)$^{-1/2}$
φ = 0.06 rad

$\pi^+\pi^-$ system:
$|B/A| = 0.54 \pm 0.01^{\mathrm{stat}} \pm 0.02^{\mathrm{syst}}$ (GeV/c^2)$^{-1/2}$
$\varphi = 1.46 \pm 0.11^{\mathrm{stat}} \pm 0.07^{\mathrm{syst}}$ rad

Azimuthal anisotropy - polarization

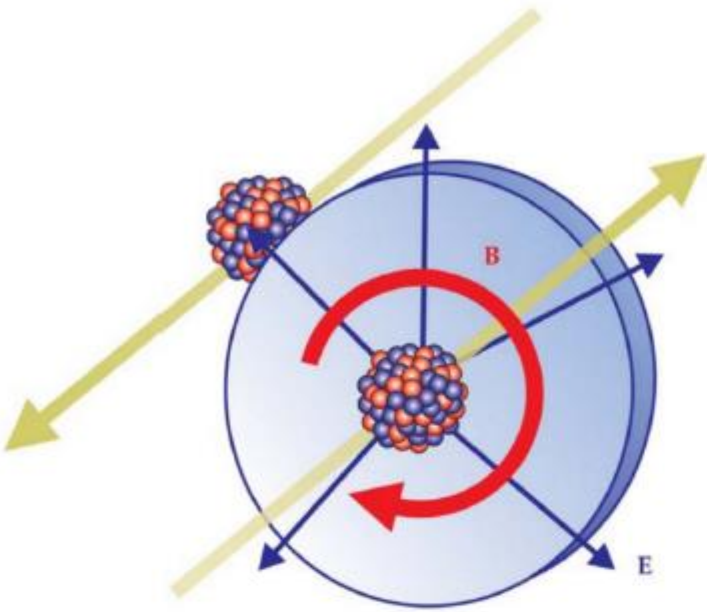

- EM field of the nuclei is highly Lorenz contracted
  - ⇒ Exchanged photons are fully linearly polarized along the impact parameter
- The polarization is transferred to the ρ^0
- ρ^0 is short lived and decays
  - ⇒ Polarization is transferred to the orbital angular momentum of pions
  - ⇒ The angular distribution of pions determined by the conservation of the total angular momentum

⇒ Azimuthal cos(2ϕ) modulation of decay products in the momentum distribution w.r.t. the polarization direction

⇒ But, the impact parameter is random event-by-event, so the anisotropy vanishes

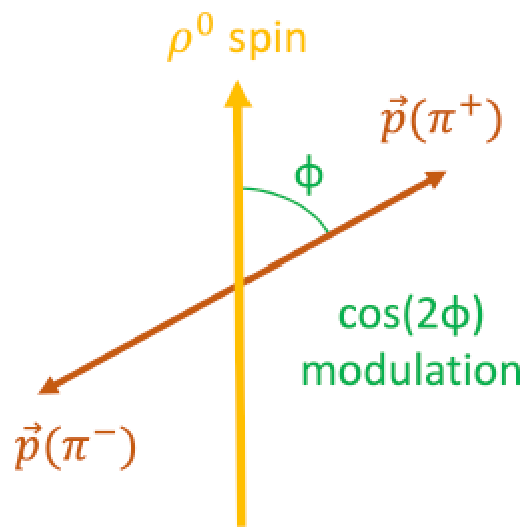

Quantum interference

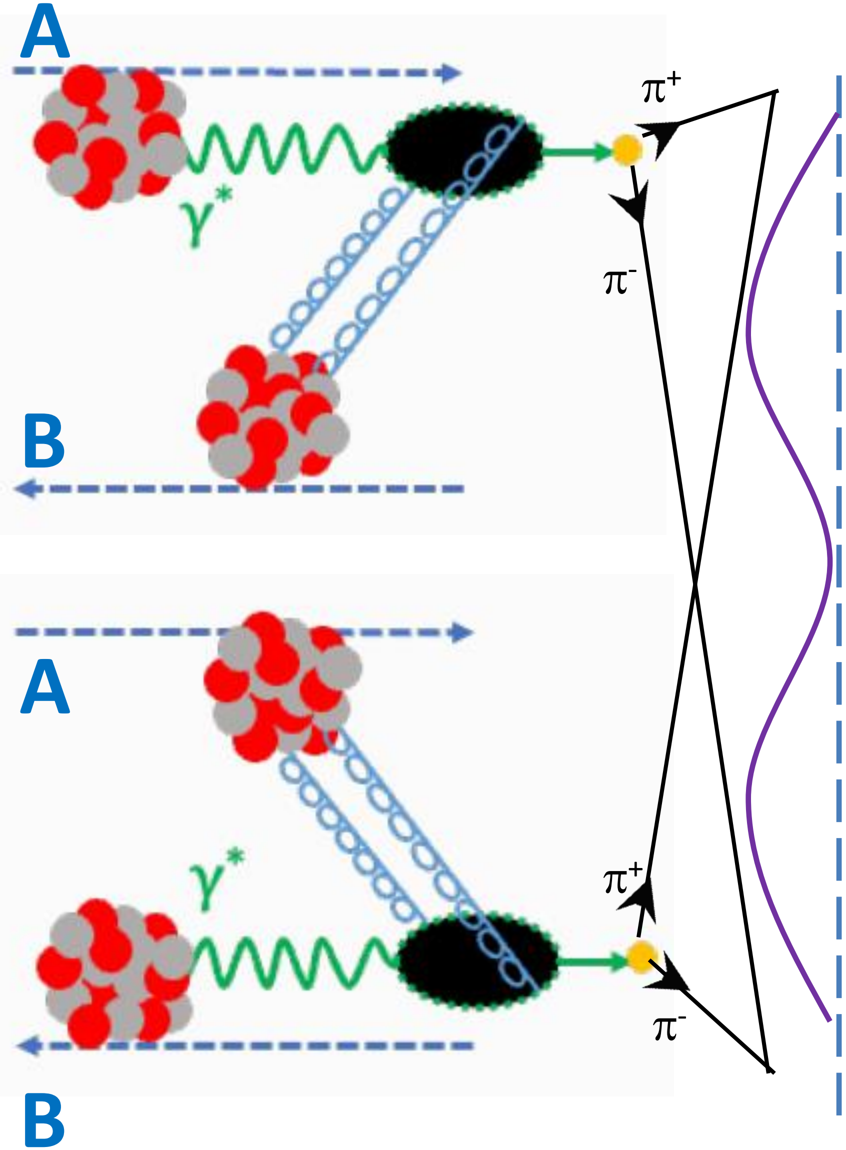

- Two indistinguishable sources (γ^*) and targets of produced VM related by parity transformation
  - Interference between amplitudes → add the amplitudes, not the cross sections
- Negative parity of VM → opposite sign of amplitude
  - $\sigma \sim |1 - e^{i\boldsymbol{p}\cdot\boldsymbol{b}}|^2$
  - Destructive interference at very low $p_T < 1/b$
  - Reduction of production cross section at small p_T
- Interference effect (correlation between ρ^0 momentum and polarization along ***b***) preserves the anisotropy

Double-slit experiment at fm scale!

ρ^0 signal in neutron emission classes

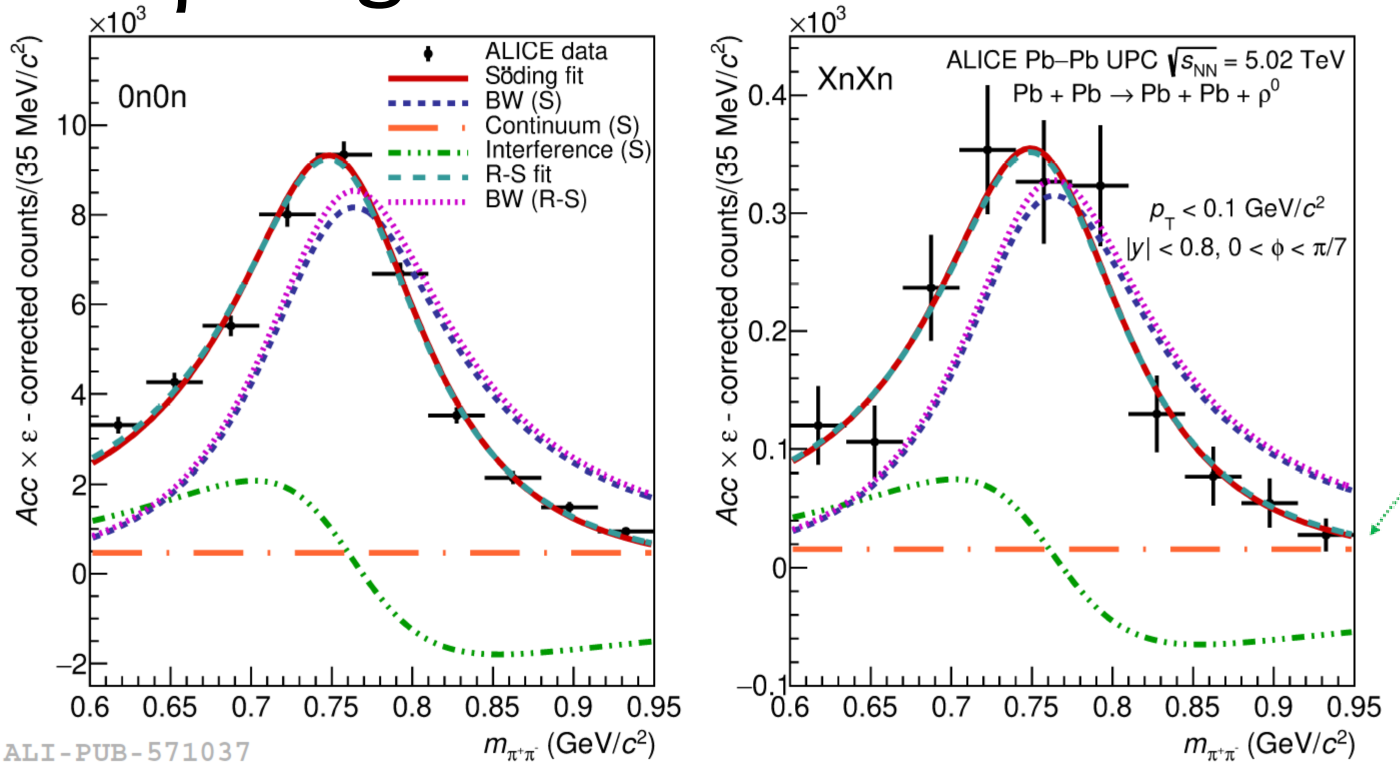

ALICE: arXiv:2405.14525, submitted to PLB

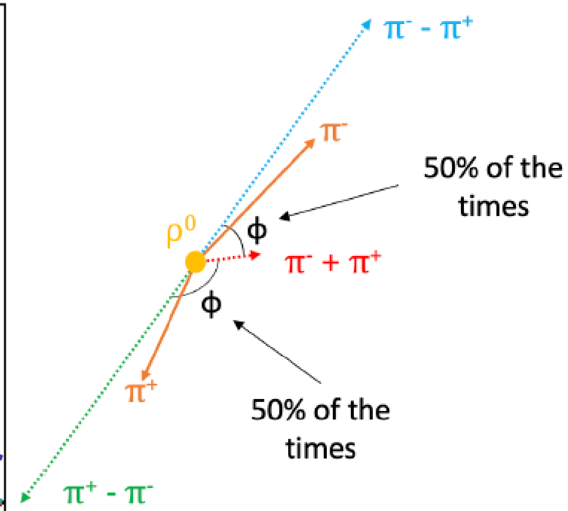

$$\vec{p}_{\pm} = \vec{p}_{T,1} \pm \vec{p}_{T,2}$$

ϕ - angle between $\vec{p}_+$ and $\vec{p}_-$

Random assignment of tracks

- 7 ϕ ranges
- 3 neutron emission classes: 0n0n, 0nXn (Xn0n) and XnXn
- Söding formula to describe resonant and non-resonant continuum pair production with the interference term (x-check Ross-Stodolsky)

Asymmetry extraction

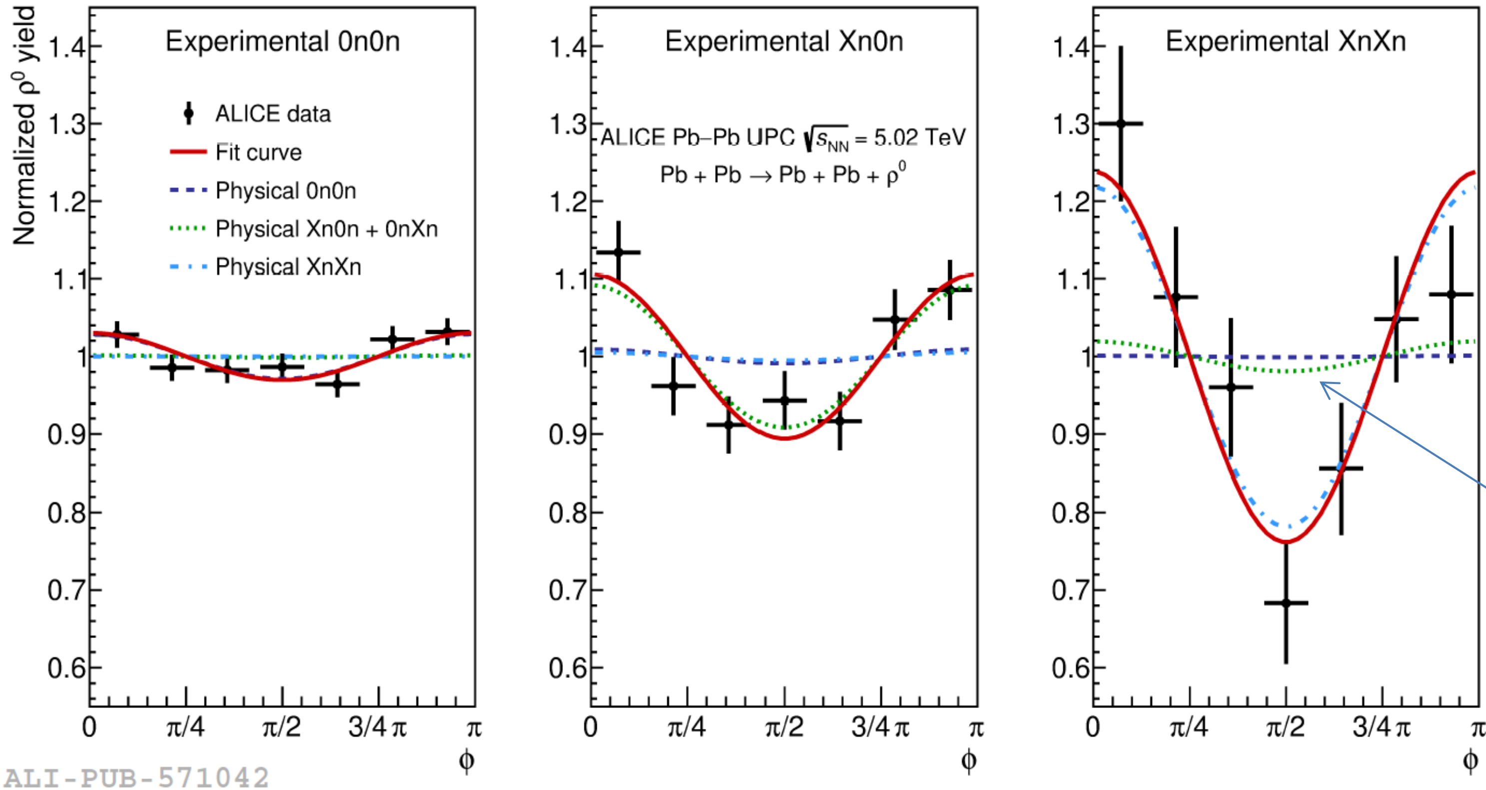

ALICE: arXiv:2405.14525, submitted to PLB

Largest effect in XnXn and Xn0n classes

Corrected for migrations across neutron classes (pile-up and ZN efficiency) → simultaneous fit in each ϕ range

Normalised ρ^0 yield — Migration matrix — True amplitudes of the modulation

$$\begin{pmatrix} n_{\rho\,\mathrm{0n0n}}(\phi) \\ n_{\rho\,\mathrm{Xn0n}}(\phi) \\ n_{\rho\,\mathrm{XnXn}}(\phi) \end{pmatrix} = \begin{pmatrix} 1 \\ 1 \\ 1 \end{pmatrix} + \begin{pmatrix} w_{\mathrm{0n0n}\to\mathrm{0n0n}} & w_{\mathrm{Xn0n}\to\mathrm{0n0n}} & w_{\mathrm{XnXn}\to\mathrm{0n0n}} \\ w_{\mathrm{0n0n}\to\mathrm{Xn0n}} & w_{\mathrm{Xn0n}\to\mathrm{Xn0n}} & w_{\mathrm{XnXn}\to\mathrm{Xn0n}} \\ w_{\mathrm{0n0n}\to\mathrm{XnXn}} & w_{\mathrm{Xn0n}\to\mathrm{XnXn}} & w_{\mathrm{XnXn}\to\mathrm{XnXn}} \end{pmatrix} \begin{pmatrix} a_{2\,\mathrm{0n0n}} \\ a_{2\,\mathrm{Xn0n}} \\ a_{2\,\mathrm{XnXn}} \end{pmatrix} \cos(2\phi)$$

Angular anisotropy

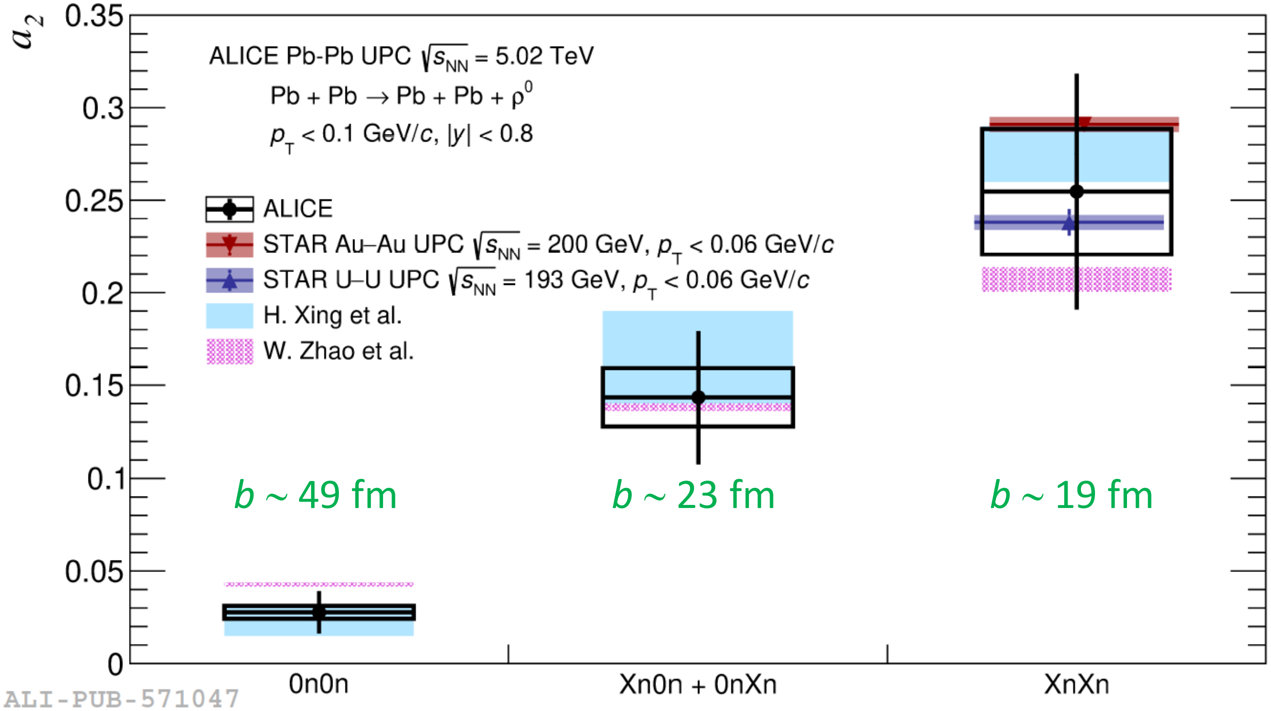

ALICE: arXiv:2405.14525, submitted to PLB

Coherently photoproduced $\rho^0 \rightarrow \pi^+\pi^-$

STAR: Sci. Adv. 9 eabq3903 (2023)

Xing: JHEP 10, 064 (2020)
Zhao: PRC 109, 024908 (2023)
- different treatment of Wilson lines (color charge density)

- First measurement of the angular anisotropy in neutron breakup classes
  ⇒ Impact parameter dependence
- The magnitude increases with decreasing impact parameter
- The strength of correlations in agreement with model calculations
  - The **anisotropy** comes from **linearly polarized photons** + **quantum interference** effect
  - Not possible to constrain models → Run 3 data will help
- XnXn amplitude in agreement with STAR results for Au-Au and U-U

Exclusive four pion photoproduction

- $\rho^0(770)$ photoproduction extensively studied in H1, ZEUS, STAR, CMS and ALICE
- Excited ρ states expected
  - The mass and the width poorly measured
- Pb Pb $\rightarrow$ Pb Pb $\pi^+ \pi^- \pi^+ \pi^-$
- Coherent component clearly seen

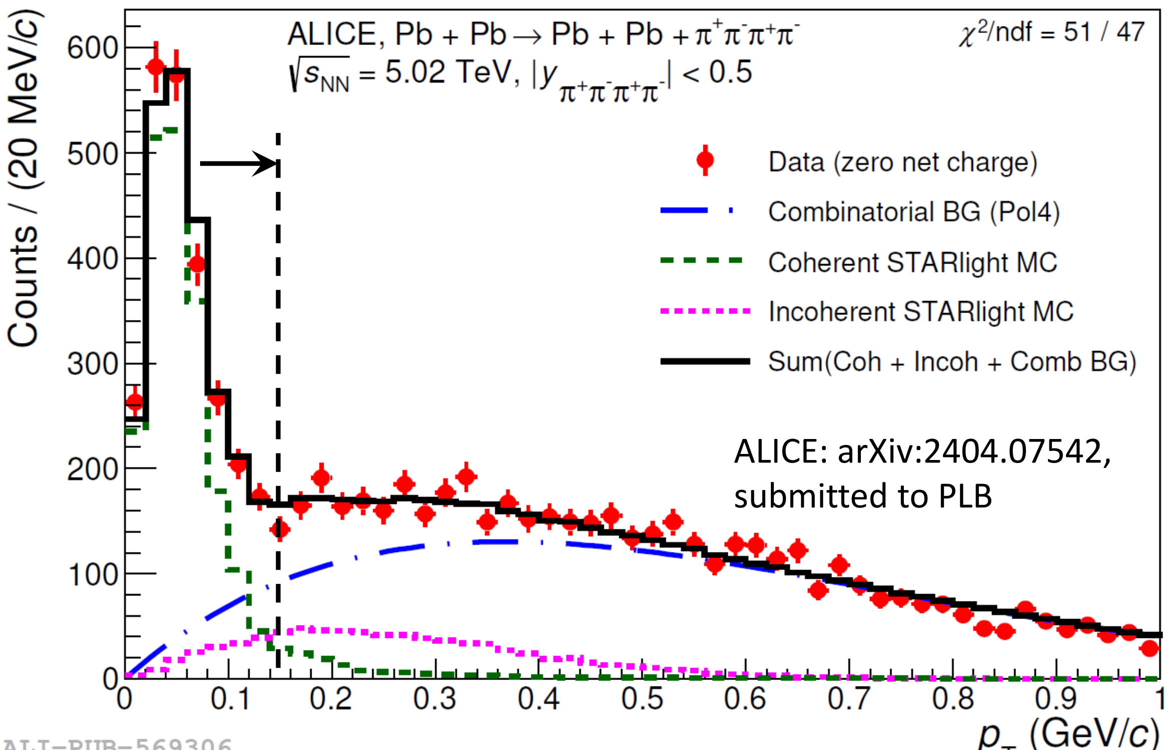

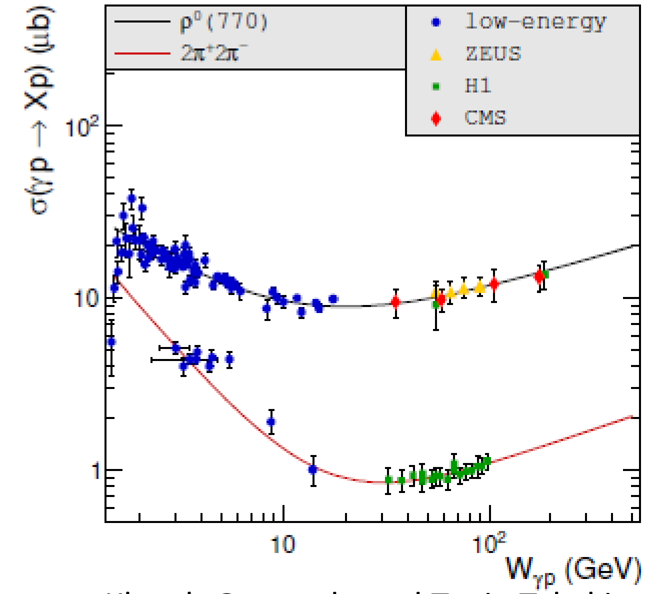

Klusek-Gawenda and Tapia Takaki, Acta Phys. Polon. B51, 6, 1393 (2020)

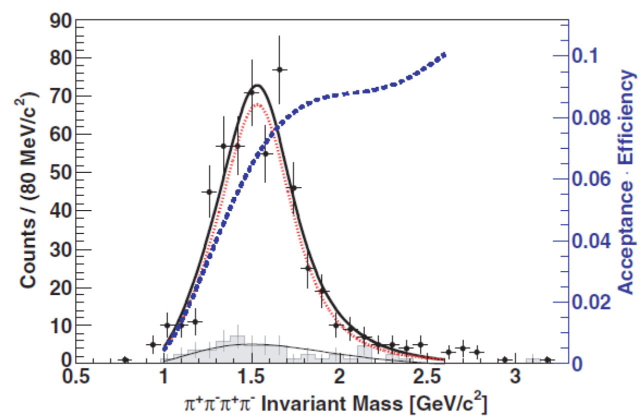

STAR: PRC 81 044901 (2010)
M = 1540 ± 40 MeV, Γ = 570 ± 60 MeV

ALICE: arXiv:2404.07542, submitted to PLB

Excited ρ resonances

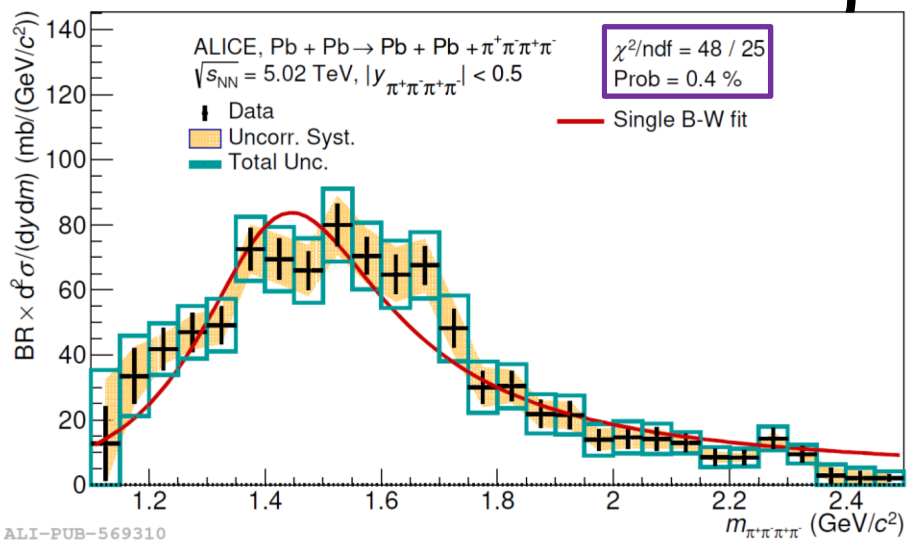

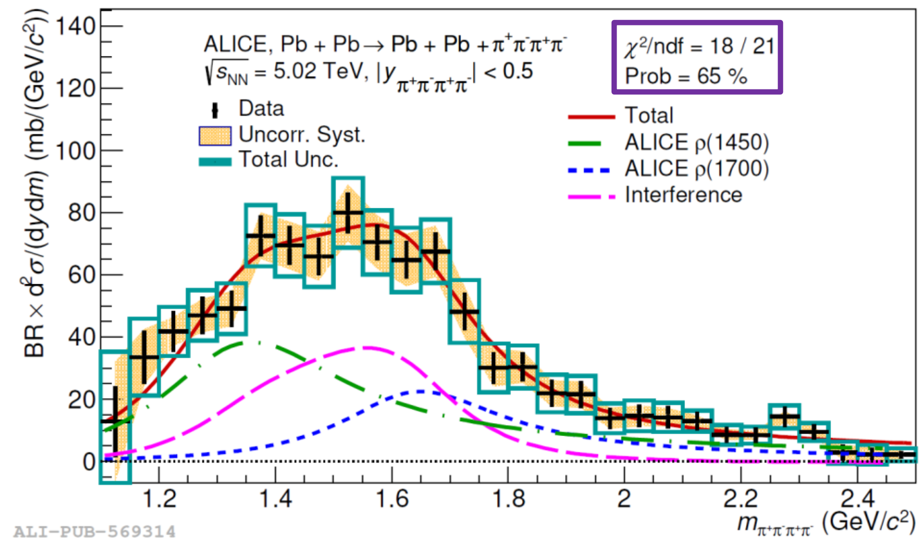

- Fully corrected invariant mass distribution fitted with a relativistic Breit-Wigner with a Söding term with one or two resonances
  - Single resonance fit in agreement with ρ(1450)
    - Disfavoured (χ^2/ndf = 48/25)
  - Two resonances fit give better description (χ^2/ndf = 18/21)
    - Rough agreement with PDG ρ(1450) and ρ(1700) with mixing angle

$$\frac{d\sigma}{dm_{\pi\pi\pi\pi}} = \left|A \cdot BW_1 + e^{-i\phi} B \cdot BW_2\right|^2$$

	m (MeV/c^2)	Γ (MeV/c^2)
PDG $\rho(1450)$	1465 ± 25	400 ± 60
PDG $\rho(1700)$	1720 ± 20	250 ± 100
STAR Au–Au	1540 ± 40	570 ± 60
ALICE Pb–Pb single resonance	$1463 \pm 2 \pm 15$	$448 \pm 6 \pm 14$
ALICE Pb–Pb $\rho(1450)$	$1385 \pm 14 \pm 36$	$431 \pm 36 \pm 82$
ALICE Pb–Pb $\rho(1700)$	$1663 \pm 13 \pm 22$	$357 \pm 31 \pm 49$
Mixing angle	$1.52 \pm 0.16 \pm 0.19$ (rad)	

Cross section × Branching ratio

- Total cross section based on single and double resonance scenario

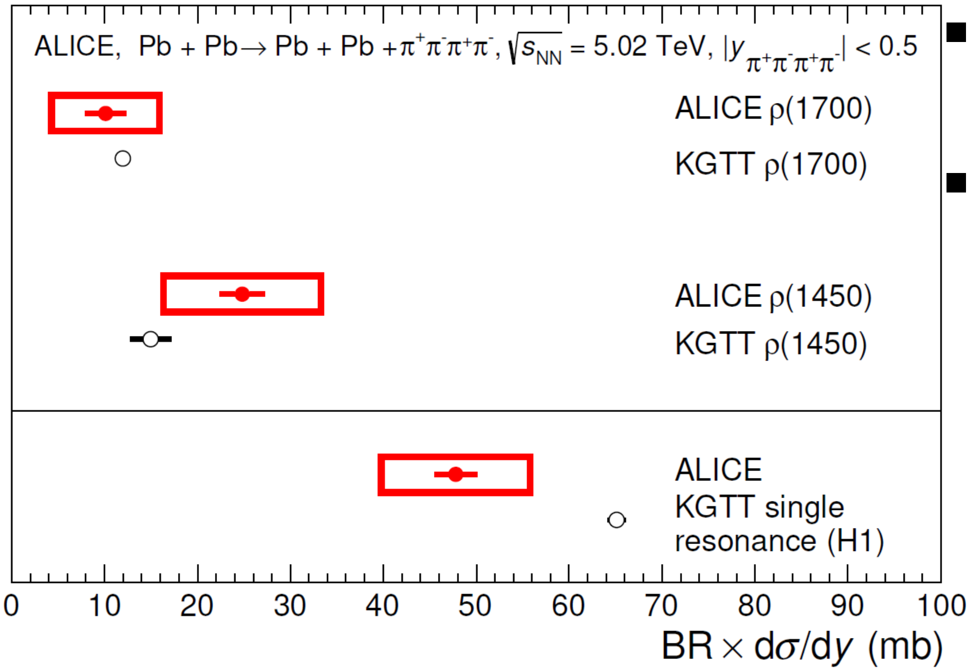

9318

ALICE: arXiv:2404.07542, submitted to PLB

- Single resonance:
  - ρ(1450): $47.8 \pm 2.3^{stat} \pm 7.7^{syst}$ mb
- Double resonance:
  - ρ(1450): $24.8 \pm 2.5^{stat} \pm 8.1^{syst}$ mb
  - ρ(1700): $10.1 \pm 2.3^{stat} \pm 5.3^{syst}$ mb

KGTT: Acta Phys. Polon. B51, 6, 1393 (2020)

- The sum of cross sections is smaller than the total one due to large interference component
- Cross sections in double resonance scenario give better agreement with theoretical calculations (KGTT) than single resonance scenario

Rapidity dependence: Ambiguity problem

$$\frac{d\sigma_{AA\rightarrow AA'J/\psi}}{dy} = N(\omega_{\gamma 1})\sigma_{\gamma A}(\omega_{\gamma 1}) + N(\omega_{\gamma 2})\sigma_{\gamma A}(\omega_{\gamma 2})$$

N – photon flux

ω_γ - photon energy

$$x_B = \frac{1}{\omega_{\gamma 1,\gamma 2}} \frac{M^2_{VM}}{2\sqrt{s_{NN}}}$$

- Two sources $\Rightarrow$ two values of x_B

High energy photon

$$\omega_{\gamma 1} = \frac{M_{VM}}{2} e^{+y}$$

Low energy photon

$$\omega_{\gamma 2} = \frac{M_{VM}}{2} e^{-y}$$

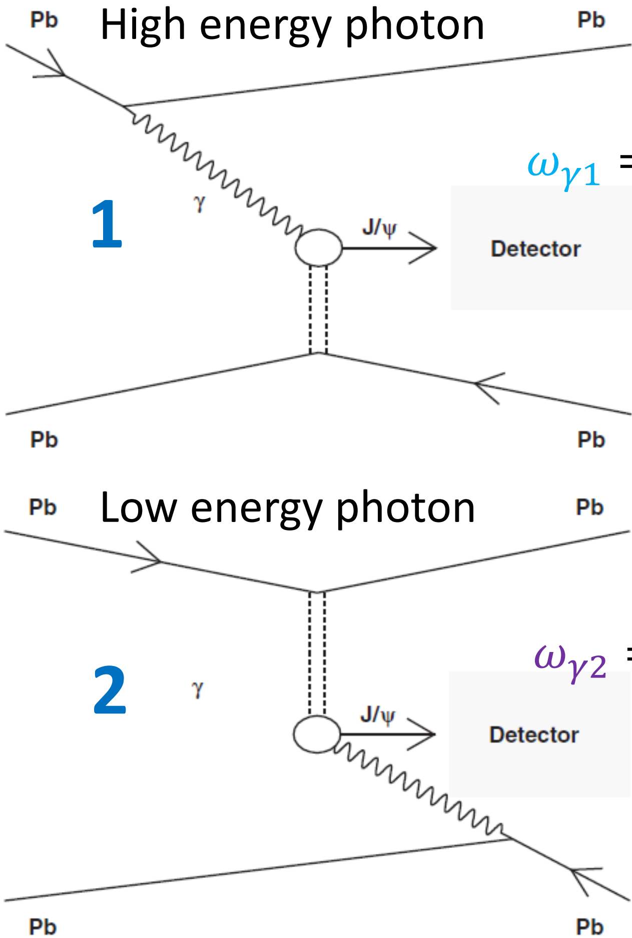

Contreras, PRC 96, 015203 (2017)

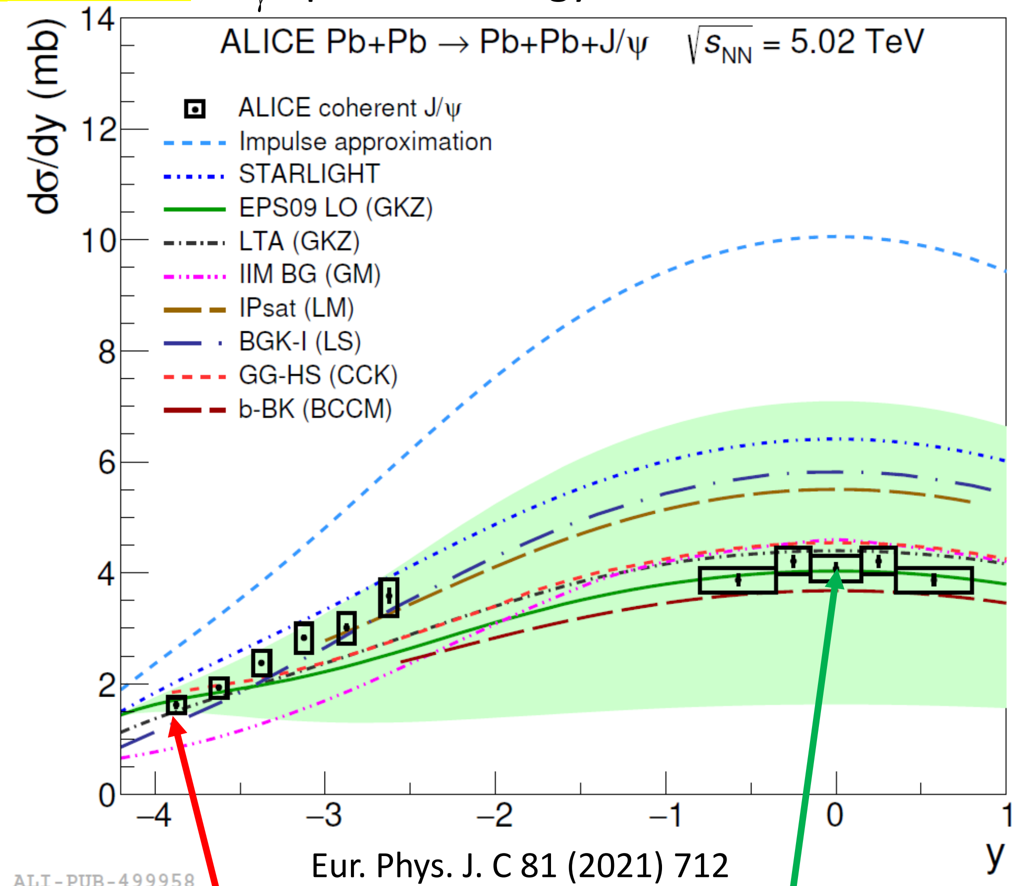

Eur. Phys. J. C 81 (2021) 712

1: 5 % $x_B \sim 1.1 \times 10^{-5}$

2: 95 % $x_B \sim 3.3 \times 10^{-2}$

50 % each $x_B \sim 10^{-3}$

How to solve the x_B ambiguity?

$$\frac{d\sigma_{AA\to AA'J/\psi}}{dy} = N(\omega_{\gamma 1})\sigma_{\gamma A}(\omega_{\gamma 1}) + N(\omega_{\gamma 2})\sigma_{\gamma A}(\omega_{\gamma 2})$$

N – photon flux
ω_γ - photon energy

- Breakup class ↔ impact parameter dependence
- Different breakup classes using the neutron ZDC on the A and C side
- Photon flux depends on the impact parameter
- Solving the linear equations resolves the two-fold ambiguity for VMs at y ≠ 0

S. Klein, P. Steinberg, Annu. Rev. Nucl. Part. Sci. 70(1), 323 (2020)

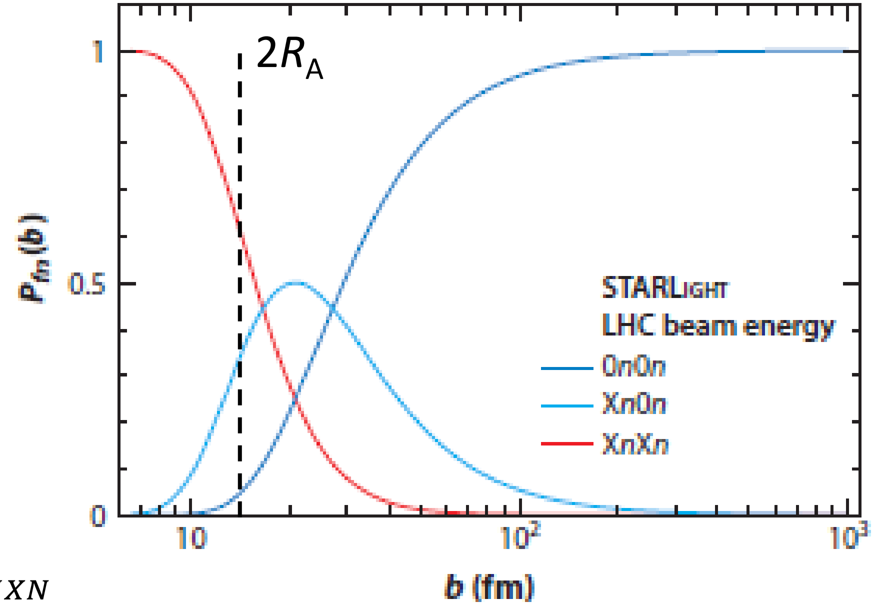

$$\frac{d\sigma_{PbPb}}{dy} = \frac{d\sigma_{PbPb}{}^{0N0N}}{dy} + 2\frac{d\sigma_{PbPb}{}^{0NXN}}{dy} + \frac{d\sigma_{PbPb}{}^{XNXN}}{dy}$$

Guzey at al., Eur. Phys. J. C 74 (2014) 7, 2942

$$\frac{d\sigma_{PbPb}{}^{0N0N}}{dy} = N^{0N0N}(\omega_{\gamma 1},+y)\sigma_{\gamma Pb}(\omega_{\gamma 1},+y) + N^{0N0N}(\omega_{\gamma 2},-y)\sigma_{\gamma Pb}(\omega_{\gamma 2},-y)$$

$$\frac{d\sigma_{PbPb}{}^{0NXN}}{dy} = N^{0NXN}(\omega_{\gamma 1},+y)\sigma_{\gamma Pb}(\omega_{\gamma 1},+y) + N^{0NXN}(\omega_{\gamma 2},-y)\sigma_{\gamma Pb}(\omega_{\gamma 2},-y)$$

measured | theory | extracted

Nuclear suppression factor of coh. J/ψ

JHEP 10 (2023) 119

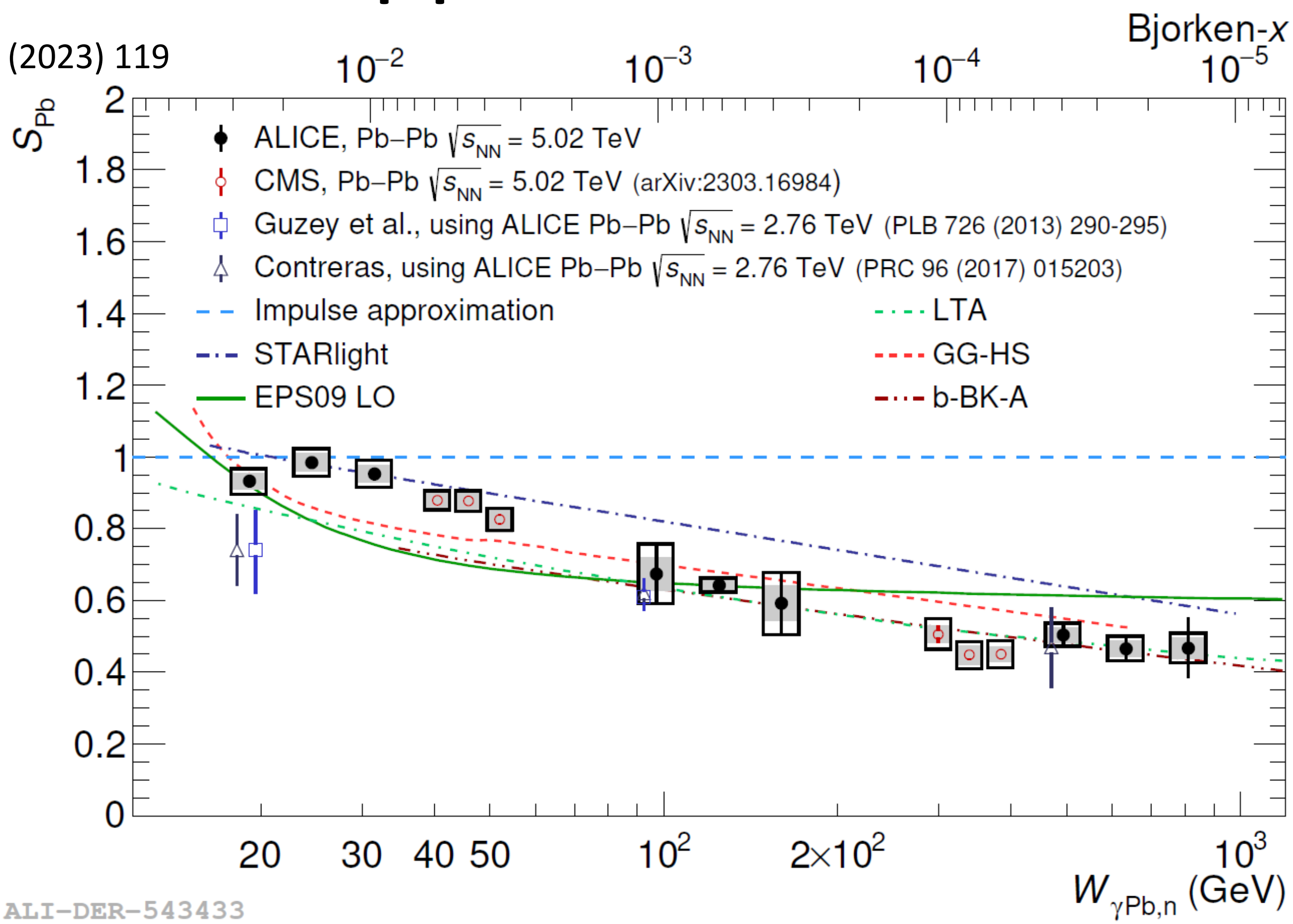

$S_{Pb} = R_g^A(x,Q^2) = g_A(x,Q^2)/Ag_p(x,Q^2)$

- At low-x_B data favours both saturation and shadowing models
- No model describes the whole energy/Bjorken-*x* range!

Coherent and incoherent J/ψ - $|t|$

- Gluon density is impact parameter *b* dependant at given Bjorken-*x* and Q^2
- *b* and p_T are Fourier conjugates
- $p_T^2 \approx |t|$- dependence of cross section constrains transverse gluonic structure at low x_B
- In Good-Walker approach
  - Coherent photoproduction is sensitive to the average spatial gluon distribution
  - Incoherent photoproduction is sensitive to the variance of the spatial gluon distribution **(quantum fluctuations)**
- Larger |t| range → scatter of smaller object

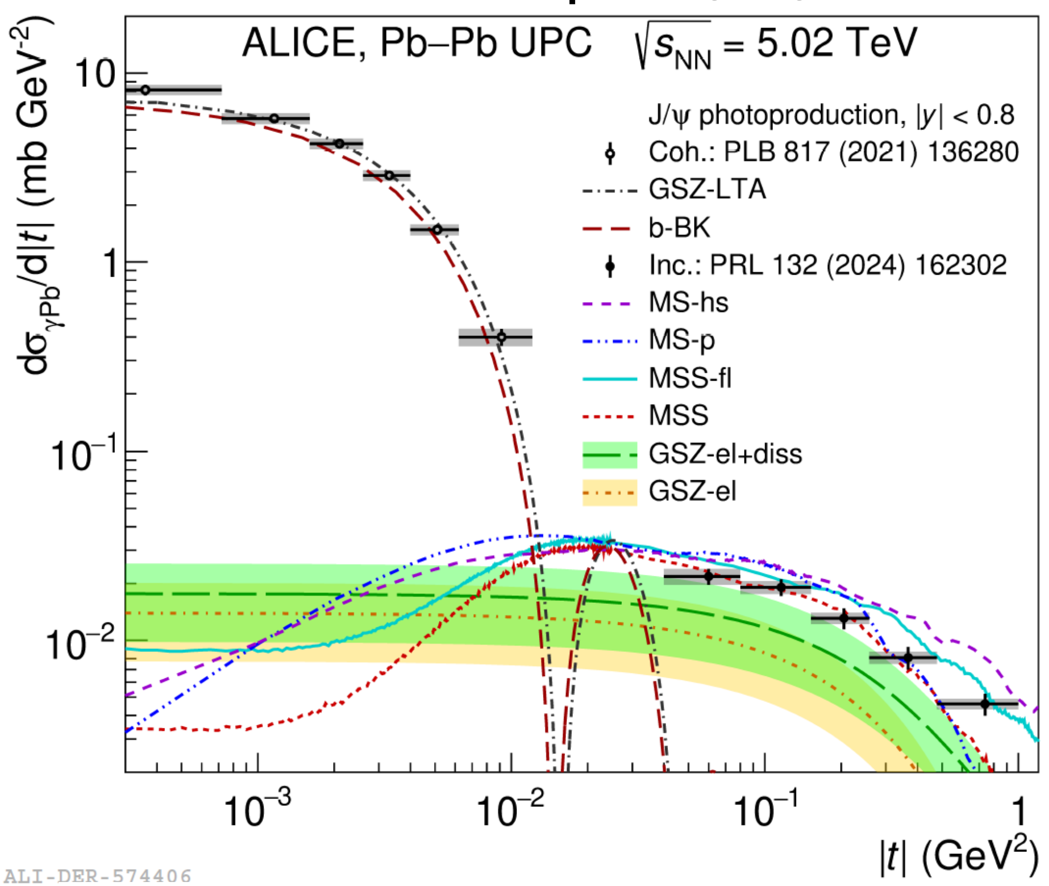

$$\frac{d\sigma^{inc}}{dt} = \frac{R_g{}^2}{16\pi}\left(\langle|A(x,Q^2,\vec{\Delta})|^2\rangle - |\langle A(x,Q^2,\vec{\Delta})\rangle|^2\right)$$

(Slope of) data favor models with gluonic subnucleon fluctuations (hot spots in MS-hs, fluctuations MSS-fl and dissociation in GSZ el+dis)

Run 3 data taking

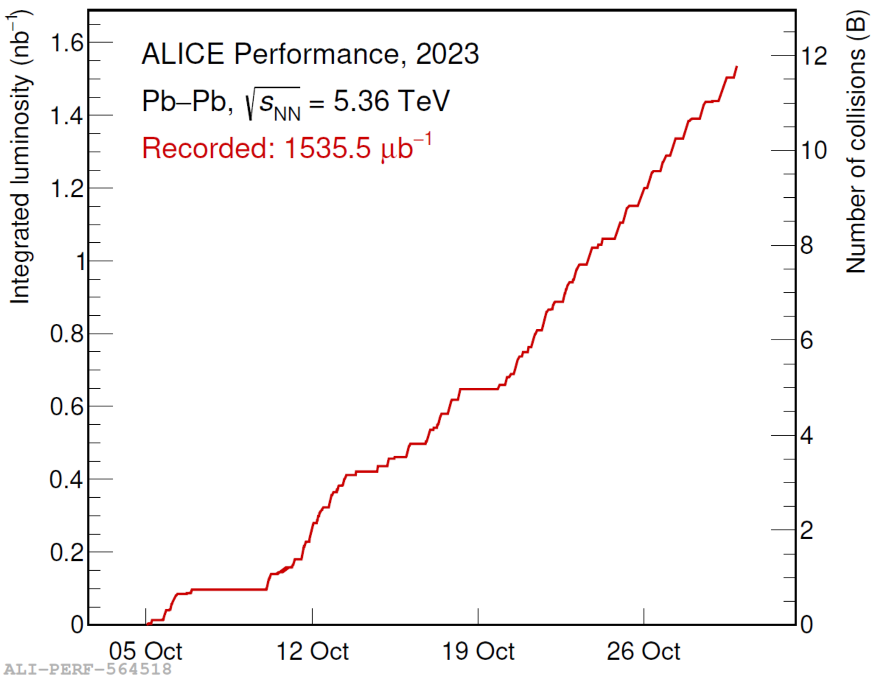

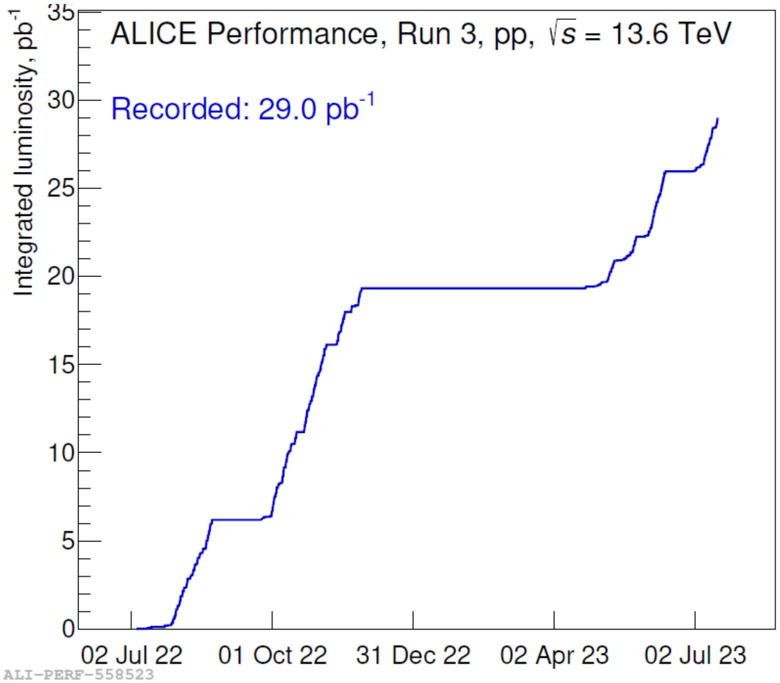

- Successful 2023 heavy-ion campaign
  - Collected luminosity ~1.6 nb^{-1} of Pb-Pb data
- Successful ALICE operational in pp at high efficiency of 95 %
  - 2022: 19.3 pb^{-1}
  - 2023: 9.7 pb^{-1}
  - 2024: 10.2 pb^{-1}

Run 3 performance (Pb-Pb)

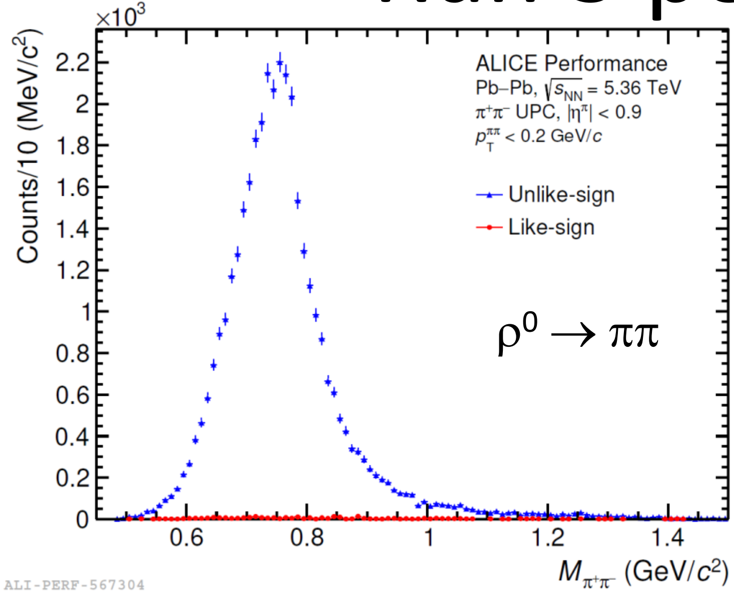

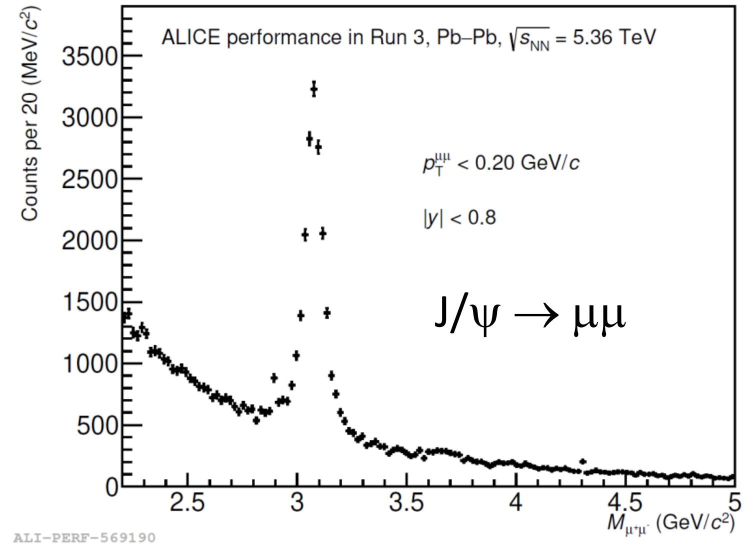

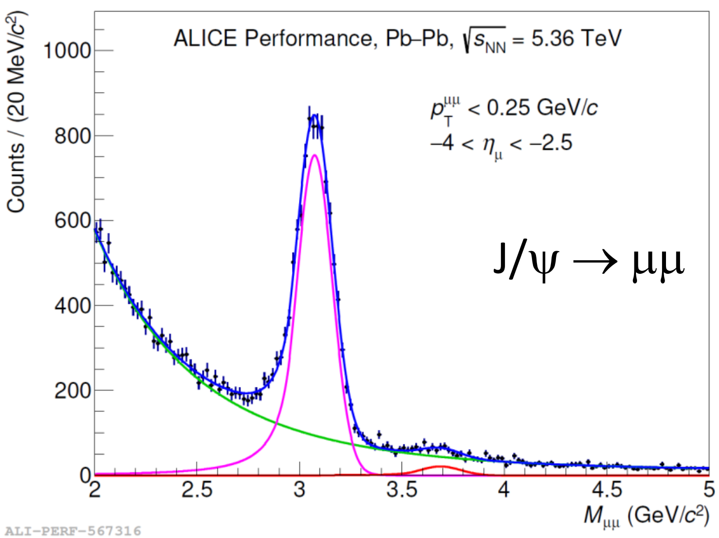

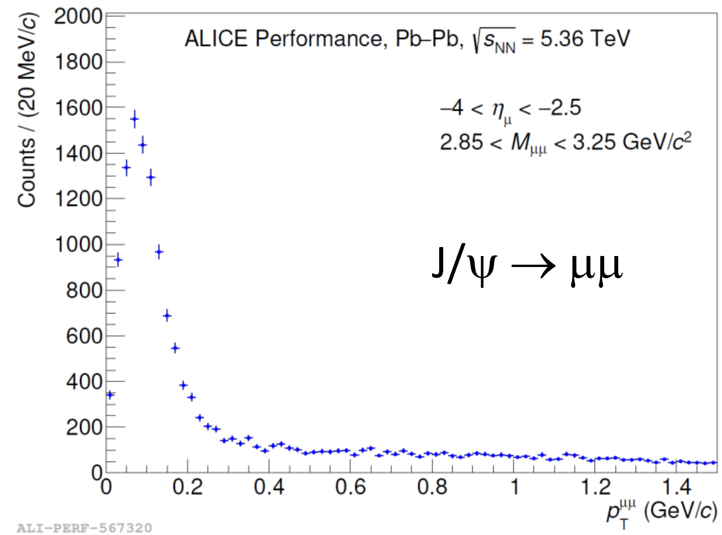

- Larger statistics available than in Run 2
- Lower invariant mass region available, no topology trigger

Run 3 performance (pp)

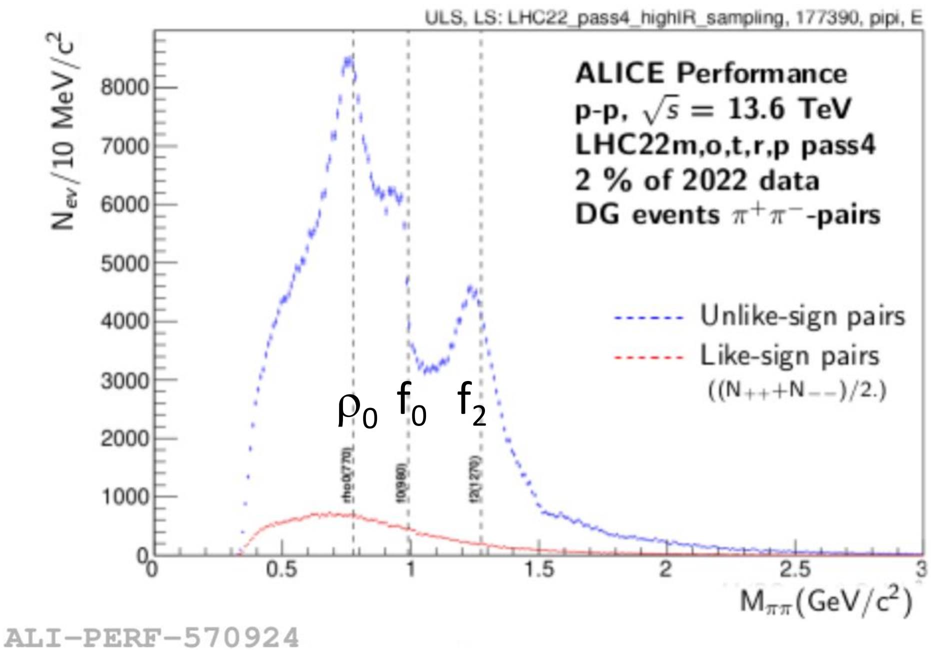

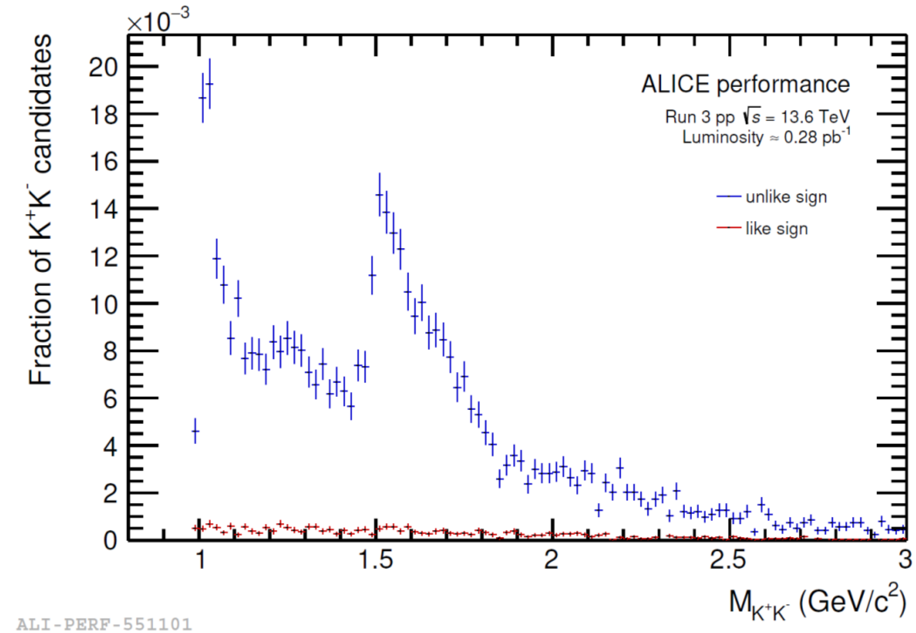

The ALICE Forward Calorimeter

- Upgrade to ALICE detector
- LOI: CERN-LHCC-2020-009
- During LS3 (2026-2029) FoCal should be installed
- $3.2 < \eta < 5.8 \rightarrow x_{\mathrm{B}} \sim 10^{-6}$
- 700 cm away from IP
- FoCal-E
- FoCal-H

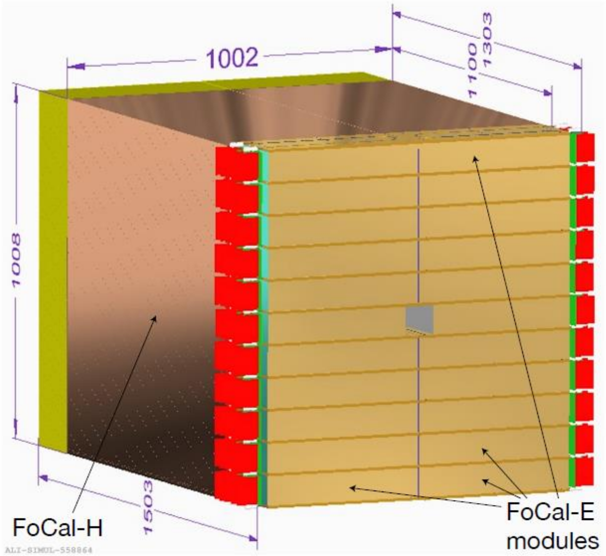

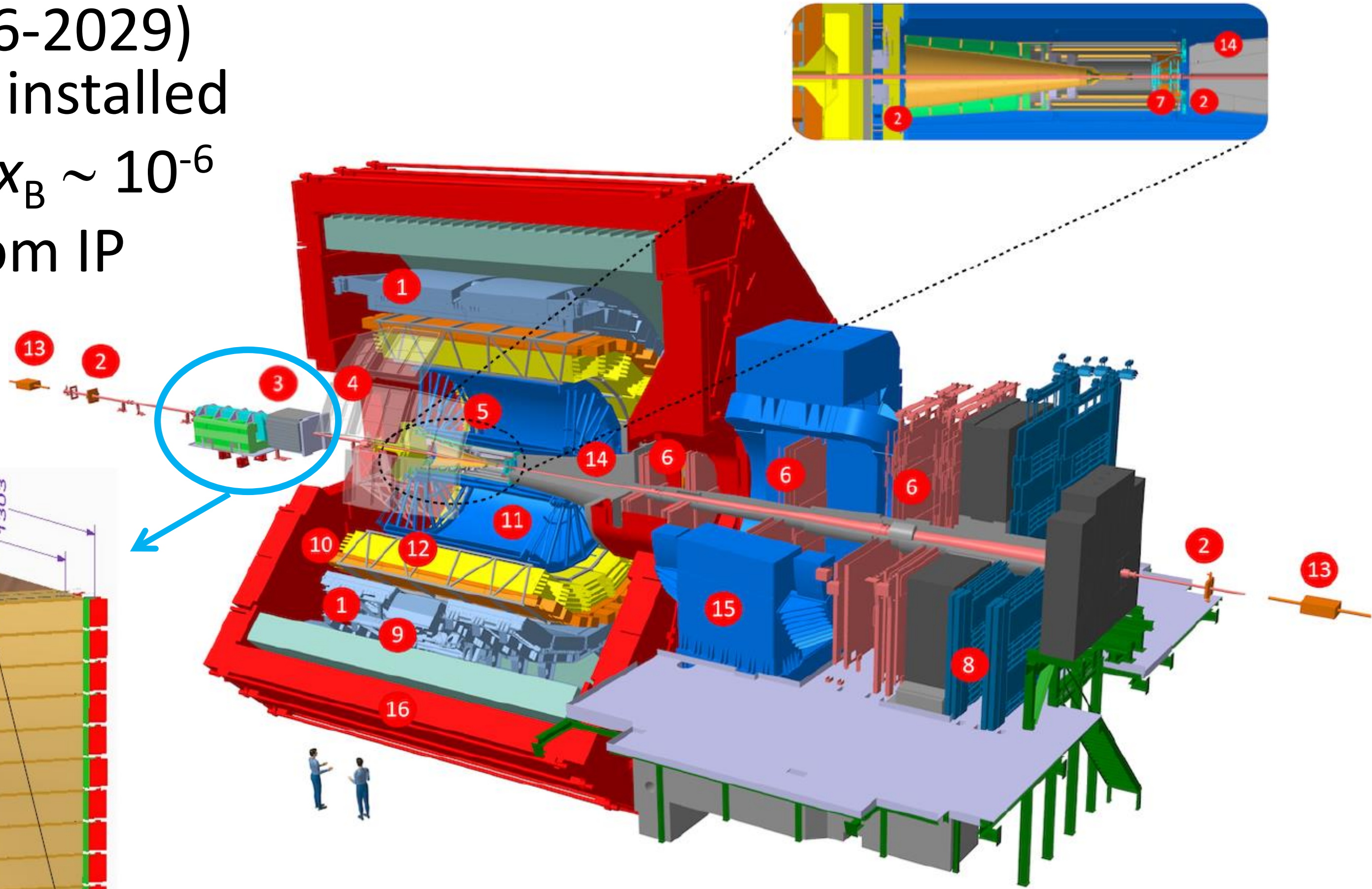

TDR aproved by LHCC

FoCal-E design

CERN-LHCC-2024-004

- Si + W sampling calorimeter
- Moliere radius $R_M^W = 0.9$ cm
- Radiation length $X_0 = 3.5$ mm
- Total depth ~ 20 X_0
- Two technologies:
  - 18 silicon pad layers of 1×1 cm^2 (LG cells)
  - 2 pixel layers of 30×30 μm^2 (HG cells)
- Channels in layers individual readout
- Weight 1650 kg
- Resolution 3%

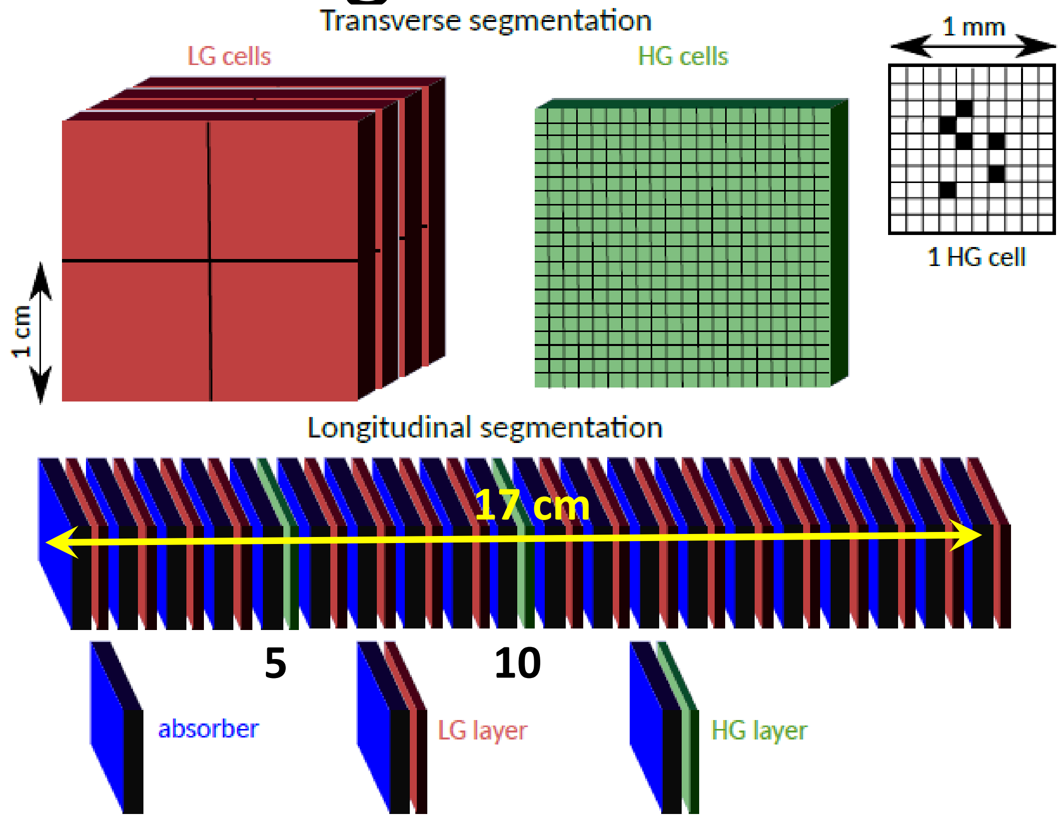

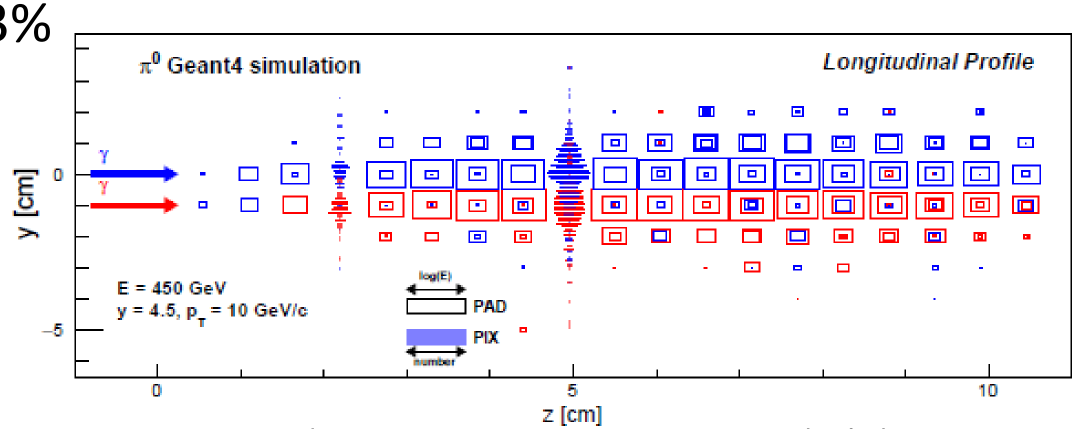

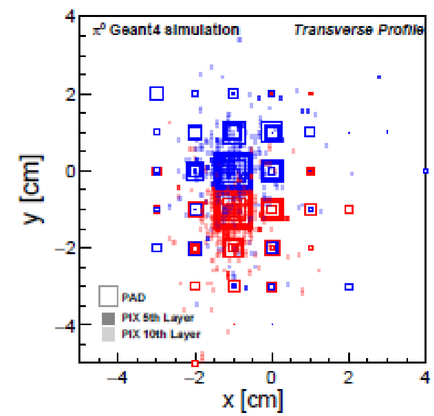

FoCal-E segmantation

- 22 modules (11 each side)
- Each module consists of 5 segments and cold plate on top
- Segment is made of 5 (4 or 2) module-layers
  - 4 pads +1 pixel
  - 4 pads
  - 2 pads

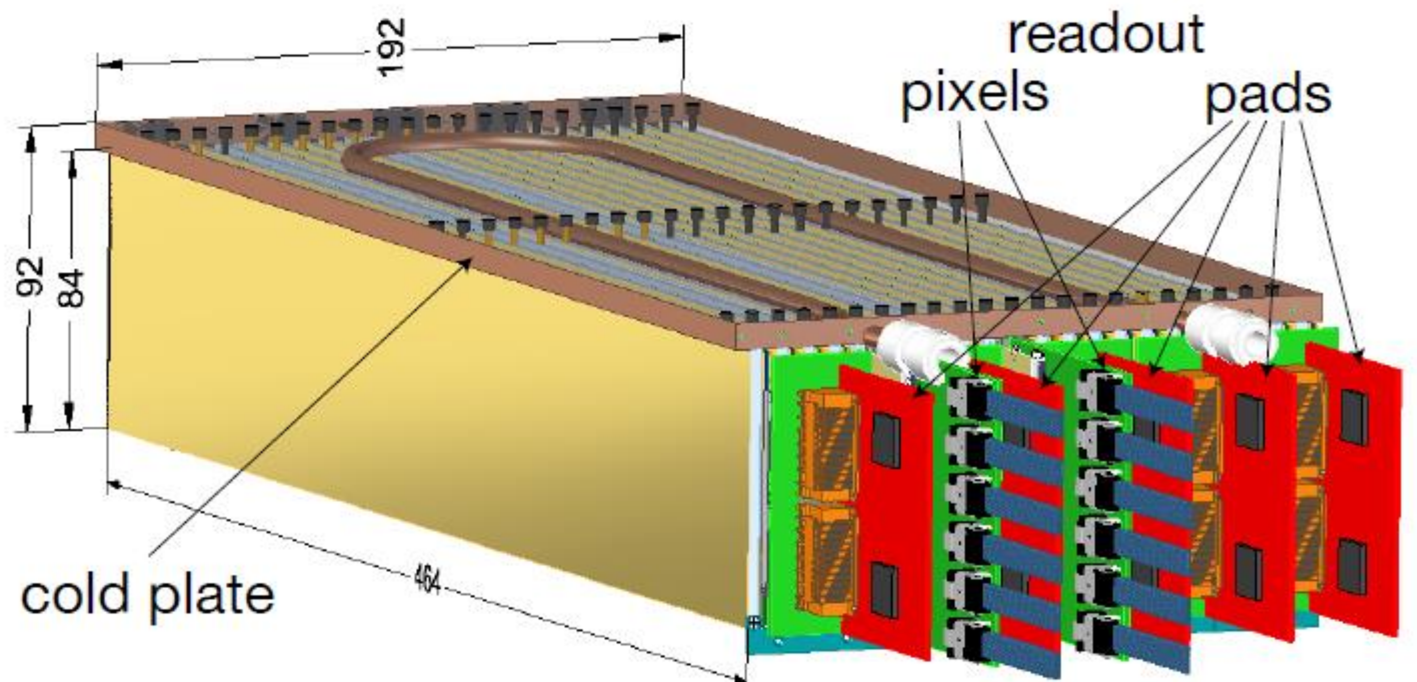

Module-layers: 5 + 5 + 4 + 4 + 2

FoCal-H design

- Hadronic scintillating-fibre calorimeter
  - Scintillation fibres embedded in Cu tubes
    - 2.5 mm outer diameter
    - 110 cm length
    - Total weigth 7000 kg
  - 224 modules
  - Designed to provide photon isolation and jet measurement
  - Capture full energy of hadronic showers inintiated in FoCal-E
  - Resolution 15%

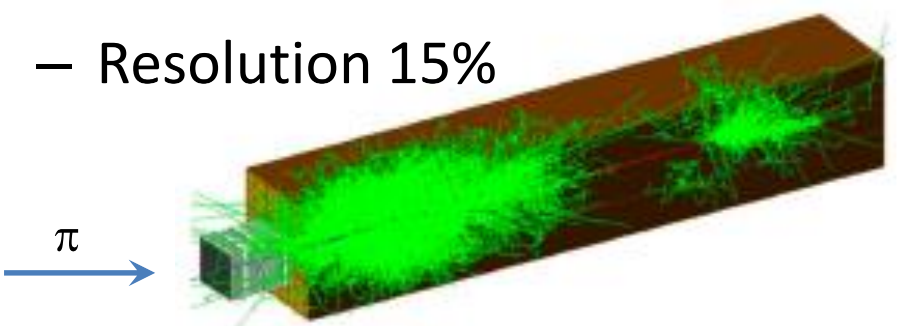

FoCal-H module

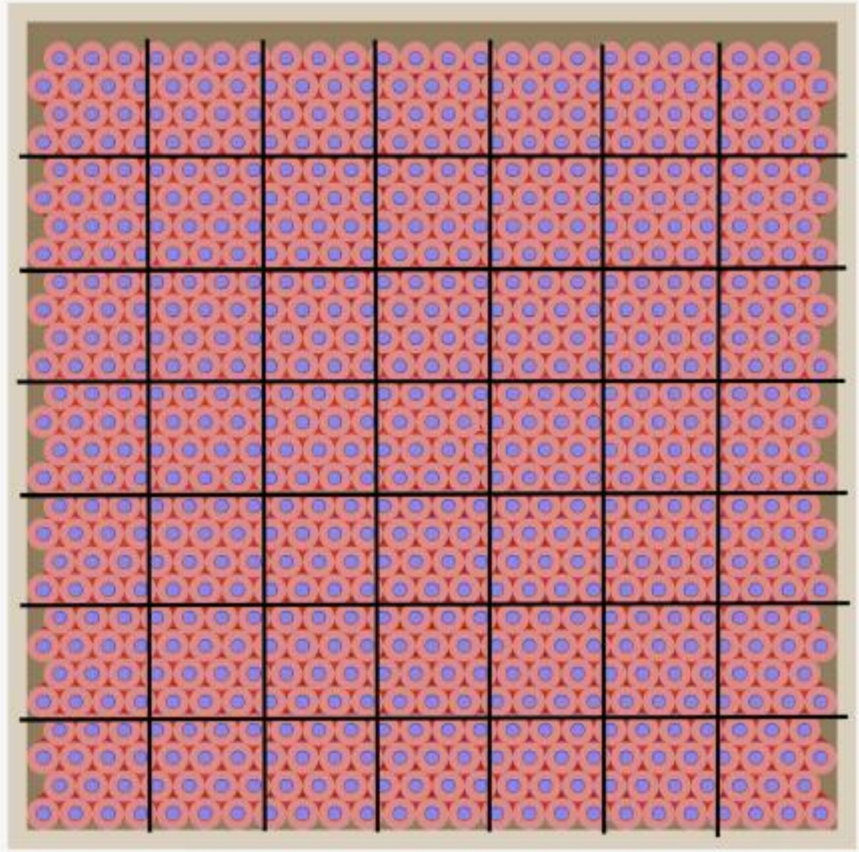

25 (24) tubes in 28 layers

Prototype tests at SPS

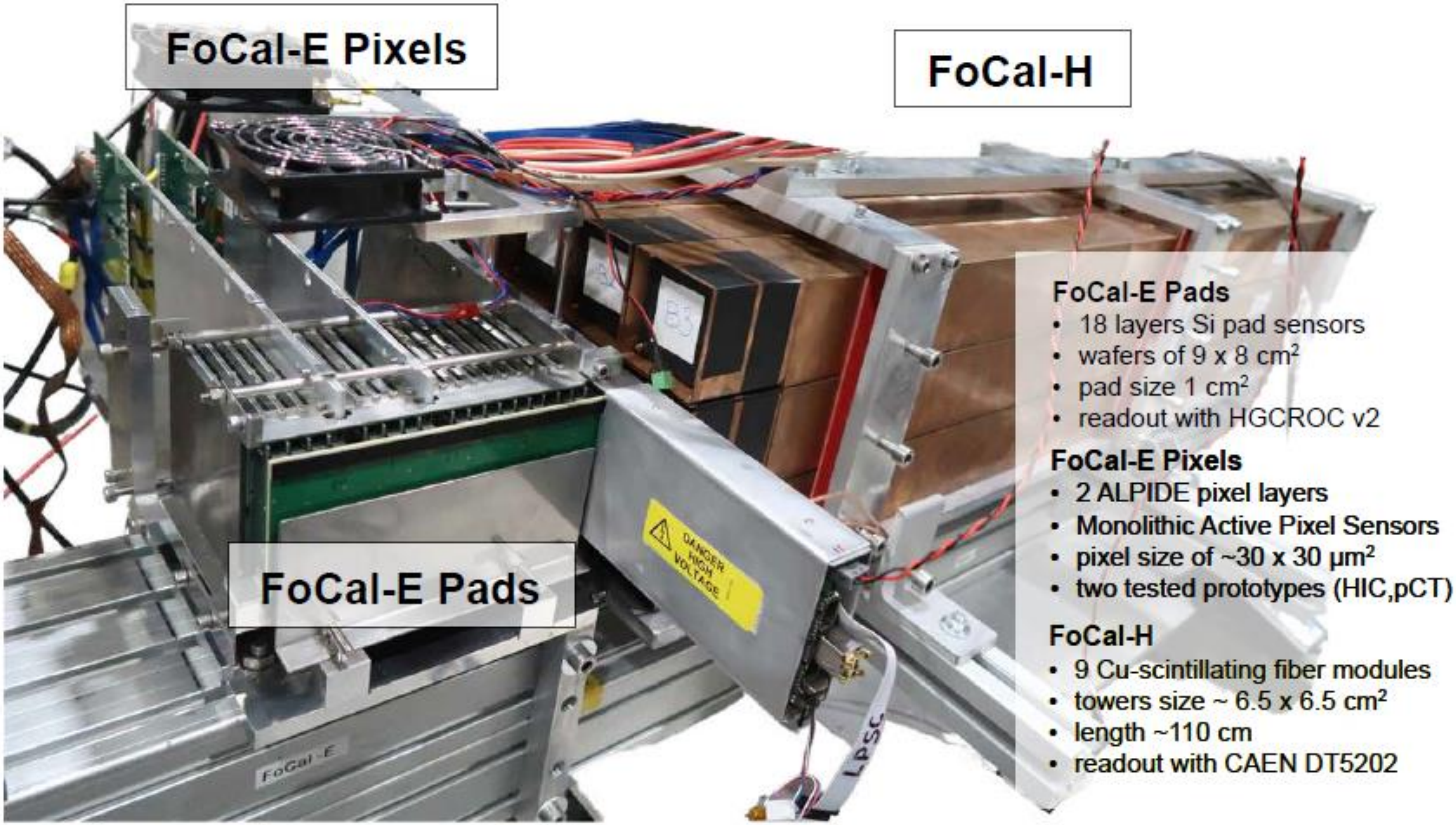

Test beam results: JINST_053P_0324

Involvement of IFJ PAN in FoCal

- IFJ PAN **responsibility**: FoCal-E cooling and FoCal assembly
- **Budget**: ~ 6M PLN (Ministerstwo Edukacji i Nauki (MEiN), DIR-WSIB.92.11.2023, 2023-2028)
- **Scientists** (3): Jacek Otwinowski, Adam Matyja, Sandor Lokos
- **Engeneers** (5): Jacek Świerblewski, Ewelina Ziółkowska, Wojciech Marek, Tomasz Cieślik, Waldemar Maciocha
- **Technicians** (5): Piotr Putek, Marek Rachwalik, Krzysztof Grzybek, Roman Wiertek, Piotr Topolski

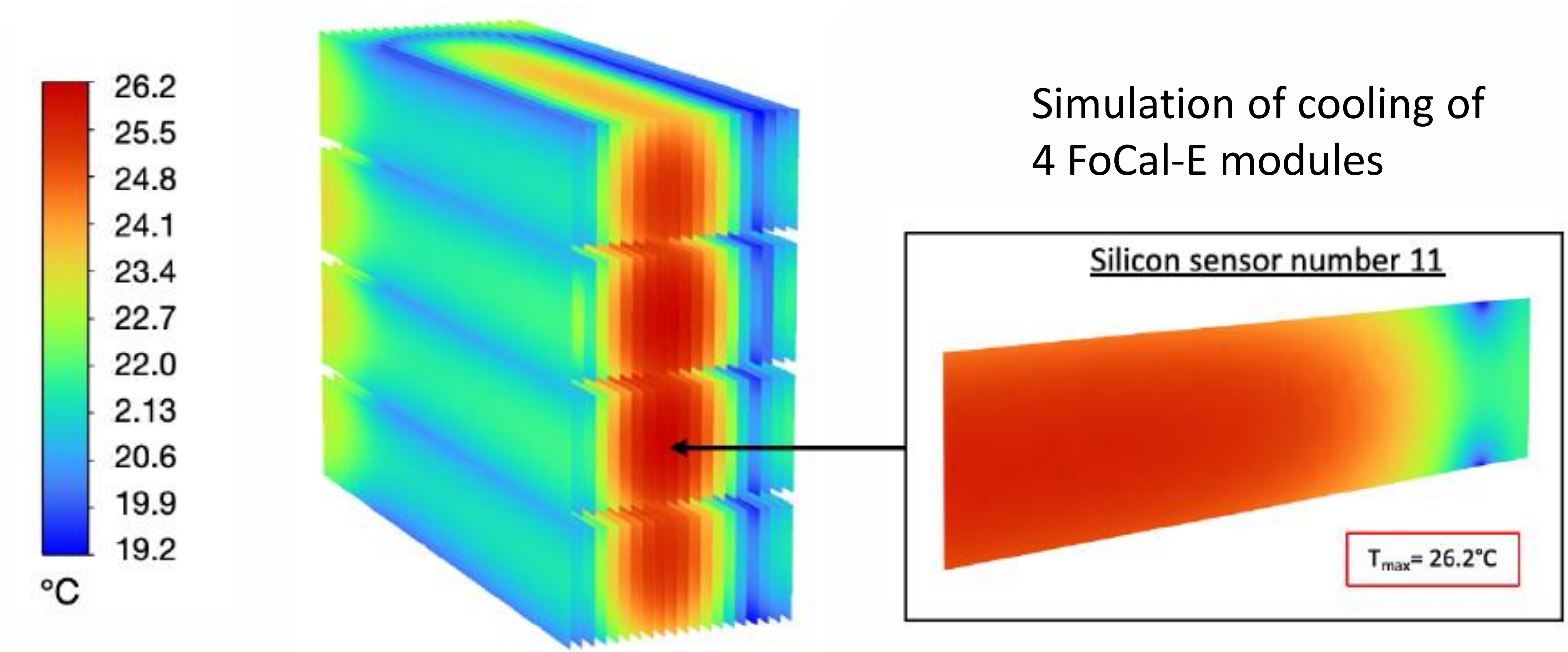

Summary

- First measurement of K^+K^- photoproduction in heavy-ion UPCs
- First measurement of the angular anisotropy in neutron breakup classes
- Measurement of cross section $\times$ branching ratio for excited ρ resonances

- First ρ^0 and J/ψ photoproduced results in UPC from Run 3
- FoCal cooling project is being implemented at IFJ PAN
- Stay tuned for new results from Run 3 and beyond!

Backup

Neutron emission in UPC

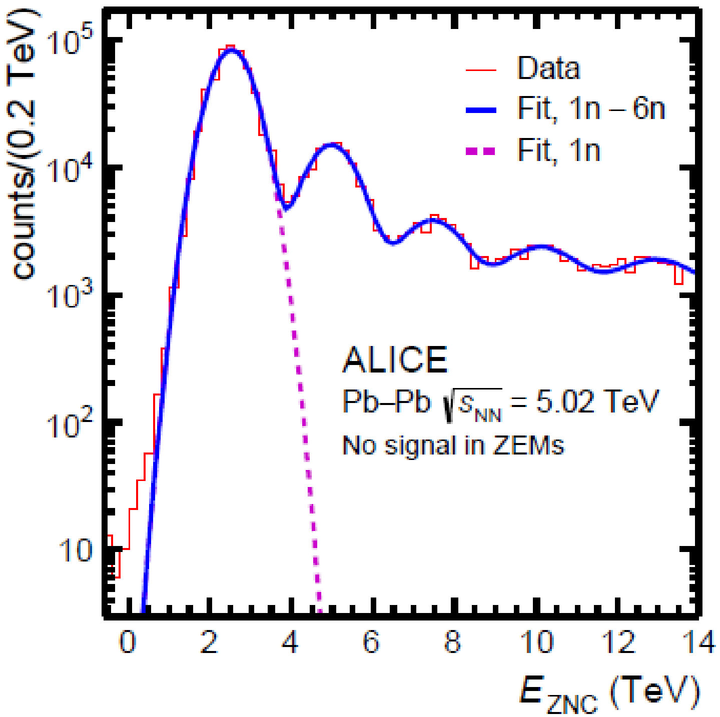

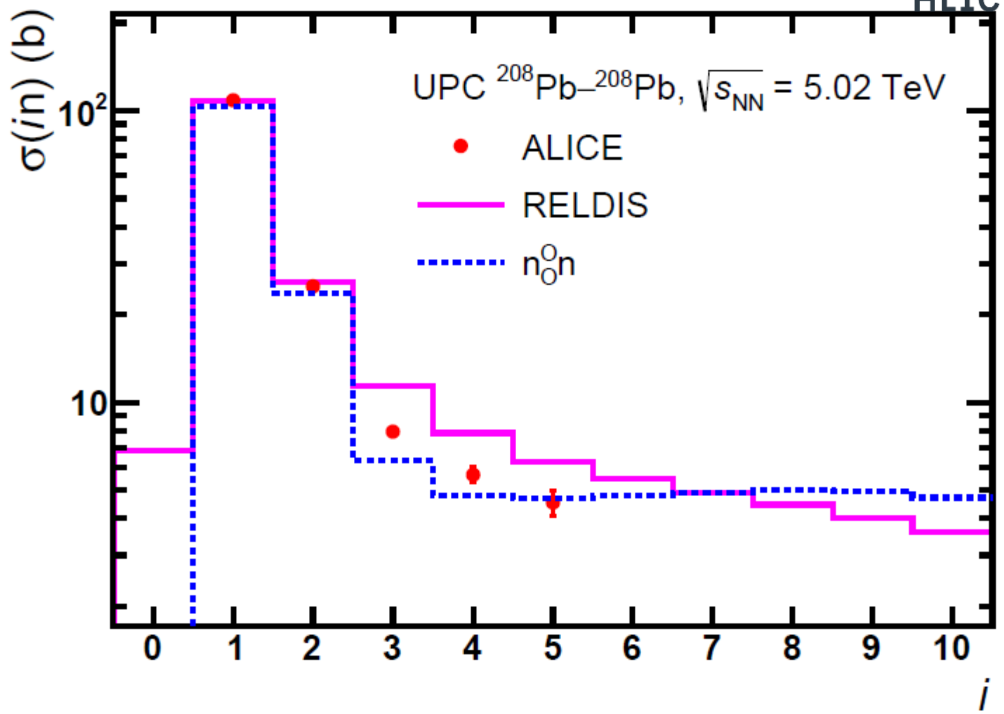

ZN	$\sigma(in)$ (b)	$\sigma^{RELDIS}(in)$ (b)	$\sigma^{n_O^On}(in)$ (b)
1n	$108.4 \pm 0.1 \pm 3.7$	108.0 ± 5.4	103.7 ± 2.1
2n	$25.0 \pm 0.1 \pm 1.3$	25.9 ± 1.3	23.6 ± 0.5
3n	$7.95 \pm 0.04 \pm 0.23$	11.4 ± 0.6	6.3 ± 0.1
4n	$5.65 \pm 0.03 \pm 0.33$	7.8 ± 0.4	4.8 ± 0.1
5n	$4.54 \pm 0.03 \pm 0.44$	6.3 ± 0.3	4.7 ± 0.1
1n–5n	$151.5 \pm 0.2 \pm 4.6$	159.8 ± 5.6	143.1 ± 2.2

ALICE, arXiv:2209.04250v1 (2022), submitted to PRC

- It is huge!
- Up to 5 neutrons
- Hadronic cross section $\sigma_{had} = 7.67 \pm 0.24$ b
- Good description of 1n and 2n emission , but other classes are not so well described

RELDIS: Phys. Part. Nucl. 42 (2011) 215.
N0ON: Comput. Phys. Commun. 253 (2020) 107181.

ρ^0 parameterization

- Söding

$$P(m_{\pi\pi}) = | A \cdot BW_\rho + B |^2$$

- Ross-Stodolsky

$$P(m_{\pi\pi}) = f \, | BW_\rho |^2 \left(\frac{m_\rho}{m_{\pi\pi}}\right)^k$$

$$BW_\rho = \frac{\sqrt{m_{\pi\pi} \, m_\rho \, \Gamma_\rho(m_{\pi\pi})}}{m_{\pi\pi}^2 - m_\rho^2 + i \, m_\rho \, \Gamma_\rho(m_{\pi\pi})} \qquad \Gamma_\rho(m_{\pi\pi}) = \Gamma(m_\rho) \, \frac{m_\rho}{m_{\pi\pi}} \left(\frac{m_{\pi\pi}^2 - 4m_\pi^2}{m_\rho^2 - 4m_\pi^2}\right)^{3/2}$$

Systematic uncertainty - anisotropy

Source	Uncertainty (%)		
	0n0n	Xn0n + 0nXn	XnXn
Signal extraction	12	9.1	13
ϕ definition	3.6	5.7	3.3
Acc $\times$ ε	2.9	0.8	0.9
ZN pile-up	0.1	2.3	0.9
ZN efficiency	0.7	0.1	0.1
Total	12.6	11.0	13.3

ALICE in future runs (3, 4 and beyond)

- Precise and new vector meson photoproduction
- Light-by-light scattering
- $(g\text{-}2)_\tau$

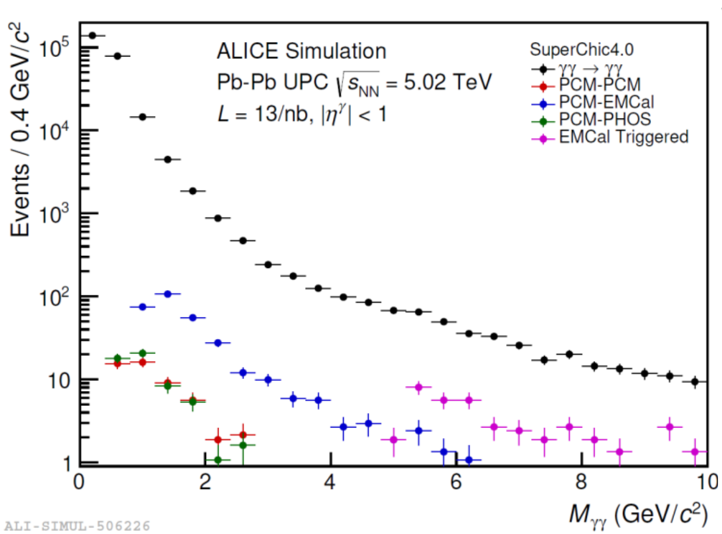

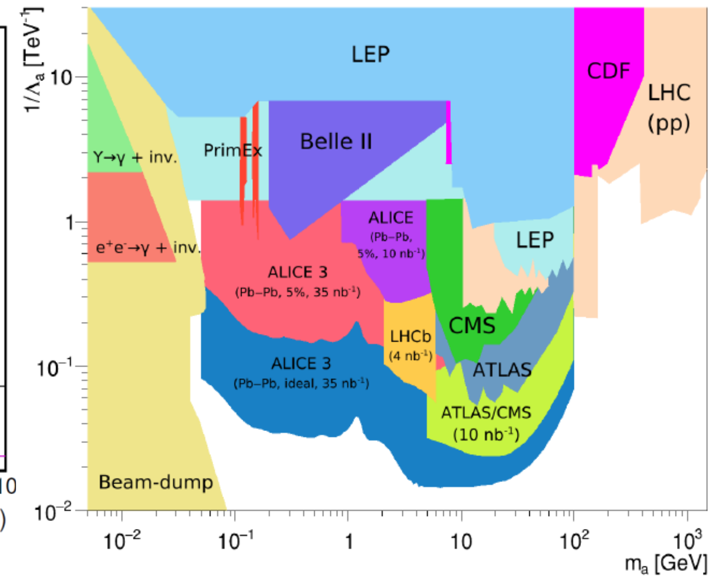

CERN Yellow Rep.Monogr. 7 (2019) 1159

Meson, channel	$\sigma^{Pb\text{-}Pb}$	N^{Tot}	$N^{\|\eta\| < 0.9}$	$N^{-4 < \eta < -2.5}$
$\rho^0 \to \pi^+ \pi^-$	5.2 b	68×10^9	5.5×10^9	-
$\rho' \to \pi^+ \pi^- \pi^+ \pi^-$	730 mb	9.5×10^9	210×10^6	-
$\phi \to K^+ K^-$	0.22 b	2.9×10^9	82×10^6	-
$J/\psi \to \mu^+ \mu^-$	1.0 mb	14×10^6	1.1×10^6	600×10^3
$\psi(2S) \to \mu^+ \mu^-$	30 μb	400×10^3	35×10^3	19×10^3
$\Upsilon(1S) \to \mu^+ \mu^-$	2.0 μb	26×10^3	2.8×10^3	880

$L^{Pb\text{-}Pb}$ = 13/nb

ALICE3 LOI: CERN-LHCC-2022-009 / LHCC-I-038